Vinylborane Formation in Rhodium-Catalyzed Hydroboration of Vinylarenes. Mechanism versus Borane Structure and Relationship to Silation

John M. Brown* and Guy C. Lloyd-Jones

Contribution from the Dyson Perrins Laboratory, South Parks Road, Oxford OX1 3QY, England

*Received February 9, 1993. Revised Manuscript Received November 18, 1993**

Abstract: Attempted catalytic hydroboration of (4-methoxyphenyl)ethene **1** with *R,R*-3-isopropyl-4-methyl-5-phenyl-1,3,2-oxazaborolidine **6** proceeded extremely slowly relative to the 3-methyl analog **2** derived from φ-ephedrine when diphosphinerhodium complexes were employed. With phosphine-free rhodium catalysts, especially the 4-methoxyphenylethene complex **7**, the reaction proceeded rapidly and quantitatively to give only the corresponding (*E*)-vinylborane **9** and 4-methoxyethylbenzene **8** in equimolar amounts. Isotopic labeling and kinetic studies demonstrated that this reaction pathway is initiated by the formation of a rhodium hydride with subsequent reversible and regiospecific H-transfer to the terminal carbon, giving an intermediate which adds the borane and then eliminates the hydrocarbon product. Further migration of the secondary borane fragment from rhodium to the β-carbon of the coordinated olefin occurs, followed by Rh–H β-elimination which produces the vinylborane product and regenerates the initial catalytic species. When the same catalytic reaction is carried out employing catecholborane in place of the oxazaborolidine, an exceedingly rapid turnover occurs. The products are again 4-methoxyethylbenzene and the (*E*)-vinylborane **23** but accompanied by the primary borane **24** in proportions which vary with the experimental conditions. None of the secondary borane, which is the exclusive product when pure $ClRh(PPh_3)_3$ is employed as catalyst, is formed. The product variation as a function of initial reactant concentration was fitted to a model in which the rhodium–borane intermediate in the catalytic cycle undergoes two competing reactions—β-elimination of Rh–H *versus* addition of a further molecule of catecholborane. The model demonstrates that a kinetic isotope effect of 3.4 operates in the β-elimination step, but none is evident in the addition of catecholborane B–D to rhodium. A similar analysis was successfully applied to the catalytic hydrosilylation of 4-methoxystyrene, with $HSiEt_3$, again employing the phosphine-free rhodium catalyst **7**; the product distribution between primary silane **29** and vinylsilane **28** was successfully predicted. The results intimate that silation (i.e., the formation of vinylsilanes under the conditions of catalytic hydrosilylation) can best be explained by a Rh–H based mechanistic model rather than the commonly assumed variant on the Chalk–Harrod catalytic cycle. They provide an explanation for the "oxygen effect" on the rate of Rh-catalyzed hydrosilylations.

Introduction

Catalytic hydroboration has attractive characteristics for organic synthesis. It commonly involves the addition of catecholborane (**HBCat**) to alkenes, for which the rate of the uncatalyzed reaction is quite low.[1] For aliphatic alkenes, the regiochemistry of the catalyzed reaction[2] follows the same trend toward anti-Markovnikov addition observed with uncatalyzed hydroboration, whereas vinylarenes exhibit a strong preference for incorporation of the boron adjacent to the aromatic ring in the catalyzed reaction but a weak or reverse preference in the uncatalyzed case. The diastereoselectivity of the catalyzed reaction with α-chiral alkenes is characteristically opposite to that observed in the uncatalyzed addition of 9-borabicyclo[3.3.1]-nonane to the same alkenes.[3] Chiral diphosphine rhodium catalysts provide an effective asymmetric synthesis of the alcohol formed on H_2O_2 oxidation of the borane from prochiral alkenes.[4]

Limited success has been obtained in catalytic hydroboration with secondary boranes other than catecholborane. The oxazaborolidines derived from ephedrine[5] and φ-ephedrine are readily prepared and give up to 78% e.e. in the Rh-catalyzed hydroboration of (4-methoxyphenyl)ethene **1** with the latter reagent **2**. Success in this reaction requires the use of a rigid chelate diphosphine complex **3** derived from 1,1-bis(diphenylphosphino)ferrocene[6] (Figure 1). The chirality of the product is derived entirely from the reagent in this case and is presumed to be caused by a direct enantioselective interaction between the coordinated alkene and the ephedrine moiety. The detailed mechanism of Rh-catalyzed hydroboration is not known,[7] but it is at least consistent with a cycle in which the addition of borane to rhodium occurs first. This provides a chiral environment which favors the coordination of the alkene *via* one rather than the other prochiral face, at the subsequent step in which a Rh-bound hydride is transferred to the β-carbon. If subsequent stages occur irreversibly this step fixes the stereochemistry. A possible model which incorporates these features is shown in Figure 2.Since the ee obtained in this reagent-controlled catalytic hydroboration was modest and modification of the oxazaborolidine structure has been productive in other areas of asymmetric catalysis, efforts were made to improve the situation by systematic structural changes. The results were unexpected and form the basis of the present work.

* Abstract published in *Advance ACS Abstracts,* January 1, 1994.

(1) Brown, H. C.; Chandrasekharan, J. *J. Org. Chem.* **1983**, *48*, 5080. Lane, C. F.; Kabalka, G. W. *Tetrahedron* **1976**, *32*, 981.

(2) Burgess, K.; Ohlmeyer, M. J. *Chem. Rev.* **1991**, *91*, 1179. Männig, D.; Nöth, H. *Angew. Chem., Int. Ed. Eng.* **1985**, *24*, 878. Cf.: Hewes, J. D.; Kreimendahl, C. W.; Marder, T. B.; Hawthorne, M. F. *J. Am. Chem. Soc.* **1984**, *106*, 5757. Sa.: Harrison, K. N.; Marks, T. J. *J. Am. Chem. Soc.* **1992**, *114*, 9220–1.

(3) Evans, D. A.; Fu, G. C.; Hoveyda, A. H. *J. Am. Chem. Soc.* **1992**, *114*, 6671–8. Burgess, K.; Cassidy, J.; Ohlmeyer, M. J. *J. Org. Chem.* **1991**, *56*, 1020. Burgess, K.; Ohlmeyer, M. J. *J. Org. Chem.* **1991**, *56*, 1027.

(4) Burgess, K.; van der Donk, W. A.; Ohlmeyer M. J. *Tetrahedron: Asymmetry* **1991**, *2*, 613. Hayashi, T.; Matsumoto, Y.; Ito, Y. *Tetrahedron: Asymmetry* **1991**, *2*, 601. Sato, M.; Miyaura N.; Suzuki, A. *Tetrahedron. Lett.* **1990**, *31*, 231.

(5) Joshi, N. N.; Srebnik M.; Brown, H. C. *Tetrahedron Lett.* **1989**, *30*, 5551. Sa.: Tlahuext H.; Contreras, R. *Tetrahedron: Asymmetry* **1992**, *3*, 727–30. Brown, J. M.; Lloyd-Jones, G. C.; Layzell, T. P. *Tetrahedron: Asymmetry* **1993**, *4*, 2151–4.

(6) Brown, J. M.; Lloyd-Jones, G. C. *Tetrahedron: Asymmetry* **1990**, *1*, 869.

(7) Evans, D. A.; Fu G. C.; Anderson, B. A. *J. Am. Chem. Soc.* **1992**, *114*, 6679–85. Westcott, S. A.; Blom, H. P.; Marder, T. B.; Baker, R. T. *J. Am. Chem. Soc.* **1992**, *114*, 8863–9.

0002-7863/94/1516-0866$04.50/0

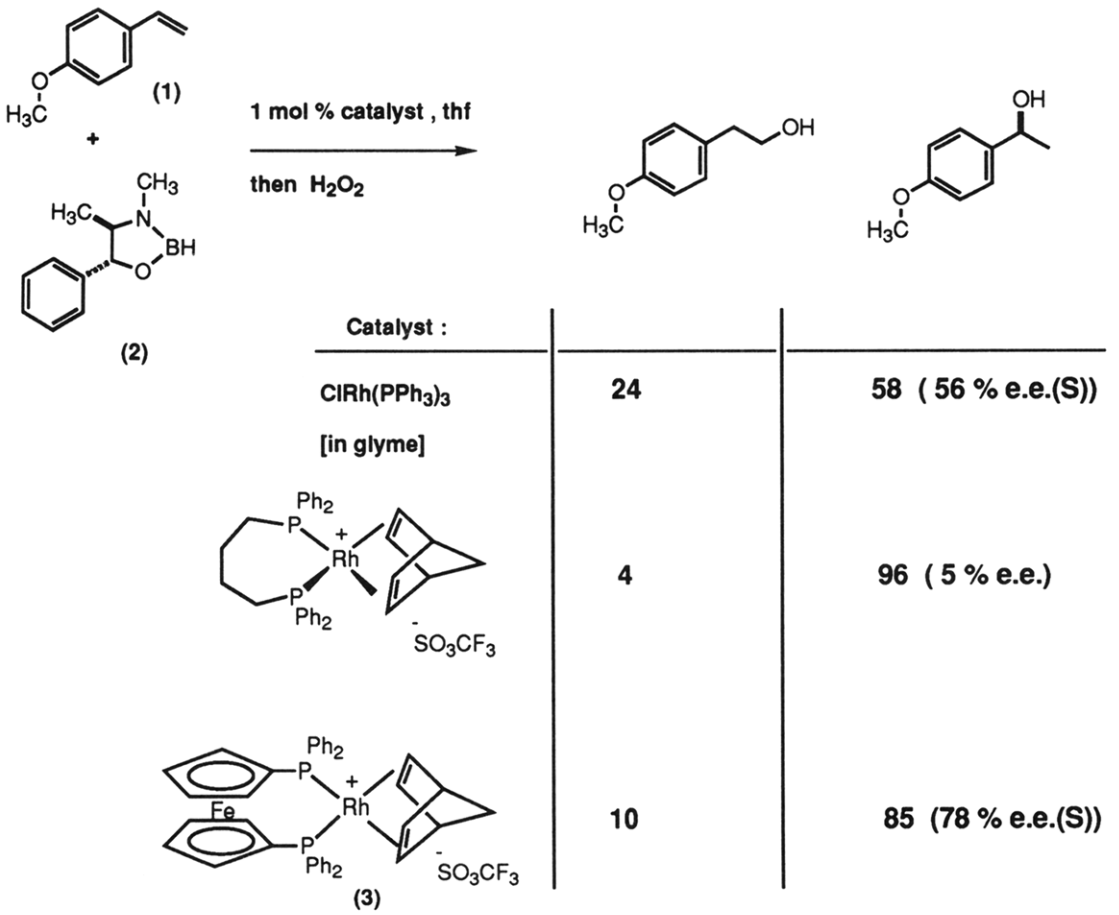

Figure 1. Catalytic hydroboration with the oxazaborolidine derived from (*R*,*R*)-ephedrine (1 mol % Rh catalyst, 0.4 mmol alkene, 0.56 mmol borane, 0.6 mL of solvent, 20 °C, 1–12 h, then 2 M NaOH, 3 M H_2O_2 1.5 mL) with different Rh catalysts. Proportions of products (remainder alkane) obtained by analysis of the ^1H NMR spectrum after oxidation are quoted; in the last case a 75% yield of secondary alcohol was obtained on a 2-g scale. Ee's were determined from the ^1H NMR of the diastereomeric mixture of (*S*)-*O*-acetylmandelate esters.

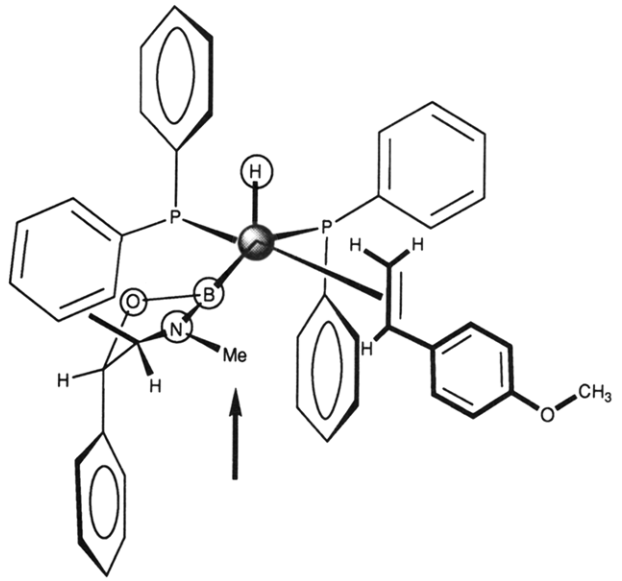

Figure 2. A model to rationalize the stereochemical course of hydroboration of alkene **1** with oxazaborolidine **2** catalyzed by Rh complex **3**, identifying potential involvement of the *N*-methyl group.

Results and Discussion

Inspection of Figure 2 indicates that the course of asymmetric hydroboration is likely to be responsive to changes in the *N*-methyl region of the ephedrine moiety and an attendant steric interaction with the bound alkene. For this reason a synthesis of the *N*-isopropyl analog was carried out, starting with 1*R*,2*R*-nor-ephedrine. A solution of the aminoalcohol **4** (40 mM) in ethanol and acetone (containing colloidal platinum *ca.* 1.4 mM) was exposed to hydrogen.[8] The reaction was monitored by a gas burette and also by analysis of the ^1H NMR of samples taken from the reaction mixture. After 18 h at ambient temperature 52 mM of hydrogen gas had reacted and ^1H NMR indicated the exclusive presence of 1*R*,2*R*-2-(*N*-isopropylamino)-1-phenylpropanol **5**. A simple filtration, evaporation, and distillation sequence afforded the product in 96% yield analytically pure. Following a procedure identical to that previously described for the preparation of oxazaborolidines,[6] 4*R*,5*R*-4-methyl-3-isopropyl-5-phenyl-1,3,2-oxazaborolidine **6** was synthesized in 82% yield as a colorless mobile oil (bp 65 °C, 0.015 mmHg; δ_B 28.4 ppm, J_{B-H} = 151 Hz). Unlike the simpler analogs, borane **6** was stable to dimerization over a period of over 9 months.[5]

Initial studies of catalytic hydroboration produced erratic results, but when freshly prepared catalyst **3** was employed in C_7D_8, there was no discernible reaction, the bright yellow solution remaining quite stable. Neither prehydrogenation of the catalyst nor UV irradiation had any effect, but when the solution was deliberately exposed to oxygen or air, reaction took place. By monitoring the ^1H NMR of a series of samples it was determined that the rate of consumption of alkene **1** was directly proportional to the amount of O_2 introduced. From the ^{31}P NMR of related samples it seemed clear that the effect of O_2 was to degrade the complex, converting the ligand into a mixture of free phosphine and its oxide. These observations prompted an attempt to catalyze the reaction employing a phosphine-free Rh catalyst **7** derived from the reactant alkene. Addition of oxazaborolidine **6** (0.237

(8) Hancock, E. M.; Cope, A. C. *Organic Syntheses*, Wiley: New York, Collect. Vol. III, pp 501–502.

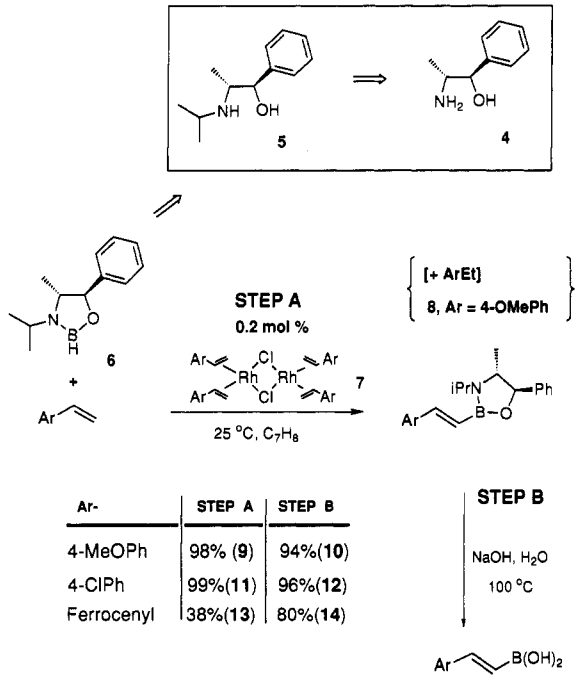

Ar-	STEP A	STEP B
4-MeOPh	98% (9)	94%(10)
4-ClPh	99%(11)	96%(12)
Ferrocenyl	38%(13)	80%(14)

Figure 3. Formation of (*E*)-vinylboranes and alkane in the reaction of alkene **1** with oxazaborolidine **6** catalyzed by phosphine-free complex **7**. Reactions were carried out on a ca. 1 mmolar scale with an alkene/borane ratio of 2.5:1. Quoted yields are of analytically pure products. The upper inset shows the synthetic precursors to **6**.

mmol) to a C_7D_8 solution of rhodium complex **7** (1.93 μmol) and (4-methoxyphenyl)ethene **1** (0.373 mmol) at ambient temperature resulted in complete conversion of the alkene into two products in exactly 1:1 ratio over a few minutes. The first was the alkane **8** and the second vinylborane **9**, which was fully characterized after reaction on a preparative scale. The ^1H NMR of the latter in C_7D_8 was informative, with the olefinic protons straddling the aromatic region at 6.55 and 7.89 ppm (^3J = 18.1 Hz).

The synthetic utility of this vinylboration reaction appears to be limited to vinylarenes; other alkenes were unreactive or gave multiple products. For those limited cases where it is effective the catalytic reaction is quantitative, clean, and rapid, affording a route to both the B-vinyloxazaborolidine and to the corresponding boronic acid, as illustrated in Figure 3. This provides an alternative to the synthesis of vinylboronic acids and vinylboronates from the corresponding alkynes or otherwise,[9] although 50% of the alkene here is diverted to hydrogenation.

Mechanistic studies. Prior to the preliminary report of part of this work,[10] vinylborane formation had only previously been observed in $PdBr_2$ catalyzed addition of pentaborane and borazine to terminal alkenes by Sneddon and co-workers,[11] with the corresponding alkane observed concomitantly. In the ensuing period,[12] a comprehensive paper on the catalysis of **HBcat** hydroborations by $ClRh(PPh_3)_3$ included the boration of an allyl silyl ether leading (after oxidative workup) to the corresponding aldehyde. It was recognized that this required a vinylborane intermediate, and a mechanism was postulated which involved regiospecific Rh–B addition to the double bond of the allyl ether followed by Rh–H elimination. In recent work, boration of 2-phenylpropene was observed in competition with hydroboration,

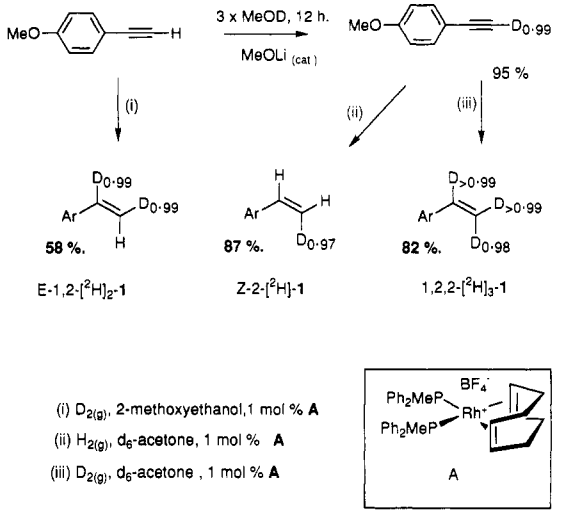

Figure 4. Synthesis of three deuterated isotopomers of alkene **1**. Atom % deuterium values quoted are from NMR analysis.

the proportion depending on the catalyst,[13] being high with $ClRh(PPh_3)_3$ (80% in total) and low with phosphine-free rhodium catalysts (2–4%). In the present study, the completely clean coproduction of vinylborane and hydrogenated product encouraged a detailed study of the reaction mechanism in which both isotopic labeling and kinetic experiments were conducted.

The synthesis of ((*E*)-1,2-[$^2H]_2$)-**1**, ((*Z*)-2-[^2H])-**1**, and (1,2,2-[$^2H]_3$)-**1** were carried out as delineated in Figure 4 employing catalytic procedures developed by Schrock and Osborn.[14] The products were isotopically homogeneous to the limits of NMR detection and MS analysis. A series of experiments were carried out with the typical protocol below.

A solution of ((*E*)-1,2-[$^2H]_2$)-**1** and oxazaborolidine **6** in C_7D_8 monitored by ^1H NMR began to react only after addition of a catalytic quantity of a stock solution of rhodium complex **7** in C_7D_8. Production of alkane **8** and vinylborane **9** was observed as concomitant H-D scrambling occurred in the parent alkene. Control experiments demonstrated that no reaction of the alkene occurred unless oxazaborolidine **6** and Rh complex **7** were both present. The 2-position of ((*E*)-1,2-[$^2H]_2$)-**1** was scrambled at a far greater rate than the 1-position exchanged. After 11 min the ^2H-distribution at the *cis*- and *trans*-2-positions was approximately equal, whilst the 1-position remained mainly deuterated. After 20 min all of the reactant alkene had been consumed; β-naphthol was added to the reaction mixture to form a relatively involatile *O*-borate[15] from residual oxazaborolidine. An essentially pure solution of (4-methoxyphenyl)ethane **8** isotopomers in C_7D_8 was then produced by vacuum distillation, and the deuterium distribution was estimated by ^1H NMR. It was established through further NMR experiments that intermolecular scrambling between undeuterated and (1,2,2-[$^2H]_3$)-**1** occurs in the presence of both oxazaborolidine **6** and catalyst precursor **7**.

Taking first the label redistribution, the results are consistent with reversible addition of a rhodium hydride, itself generated from the borane and complex **7**, to the alkene according to Figure 5. Regioselective addition to form a benzylrhodium complex is required, and a single intermediate (boxed in Figure 5) then explains both E–Z isomerization and intermolecular scrambling. An alternative but disfavored addition of Rh–H in which Rh is bound to the 2-carbon leads to some H–D exchange at the 1-position. The results are reminiscent of the reaction of H(CO)-

(9) Singleton, D. A.; Martinez, J. P.; Ndip, G. M. *J. Org. Chem.* **1992**, *57*, 5768–71. Singleton, D. A.; Martinez, J. P.; Watson, J. V.; Ndip, G. M. *Tetrahedron* **1992**, *48*, 5831–8. Cole, T. E.; Quintanalla, R.; Rodewald, S. *Organometallics* **1991**, *10*, 3777–81.

(10) Brown J. M.; Lloyd-Jones, G. C. *J. Chem. Soc., Chem. Commun.* **1992**, 710.

(11) Davan, T.; Corcoran, E. W., Jr.; Sneddon, L. G. *Organometallics* **1983**, *2*, 1693. Lynch, A. T. ; Sneddon, L. G. *J. Am. Chem. Soc.* **1989**, *111*, 6201.

(12) Burgess, K.; van der Donk, W. A.; Westcott, S. A.; Marder, T. B.; Baker, R. T.; Calabrese, J. C. *J. Am. Chem. Soc.* **1992**, *114*, 9350–9.

(13) Westcott, S. A.; Marder, T. B.; Baker, R. T. *Organometallics* **1993**, *12*, 975.

(14) Schrock, R. R.; Osborn, J. A. *J. Am. Chem. Soc.* **1976**, *98*, 2143.

(15) Brown, J. M.; Leppard, S. W.; Lloyd-Jones, G. C. *Tetrahedron: Asymmetry* **1992**, *3*, 261.

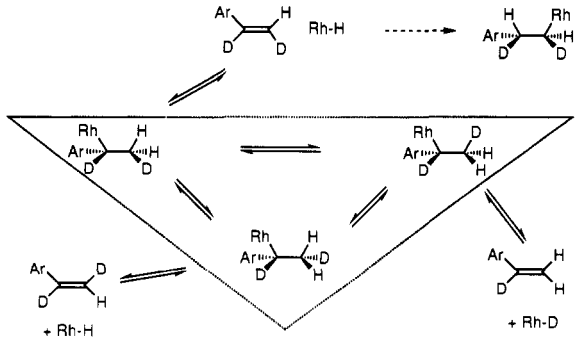

Figure 5. A rhodium hydride-based mechanism for *E*–*Z* isomerization and intermolecular label redistribution in deuterated alkene **1**.

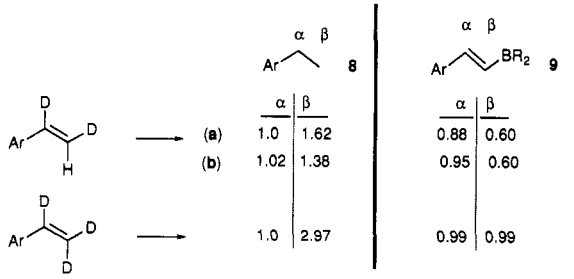

Figure 6. Isotope distribution at the sites α and β in the side chain of alkane product **8** and vinylborane product **9** from catalytic hydroboration of deuterated alkene **1** (≥0.98 D as indicated) with oxazaborolidine **6**. Reaction conditions: alkene (0.75 M), oxazaborolidine (0.47 M), and catalyst **7** (0.75 mM) in C_7D_8 for run (a) with ((*E*)-1,2-[^{2}H]$_2$)-**1** and (1.5 mM) for the other runs. Reactions were complete in approximately 20 min at 25 °C. Tabulated values refer to the total number of deuteriums at each site of product determined by ^{1}H NMR.

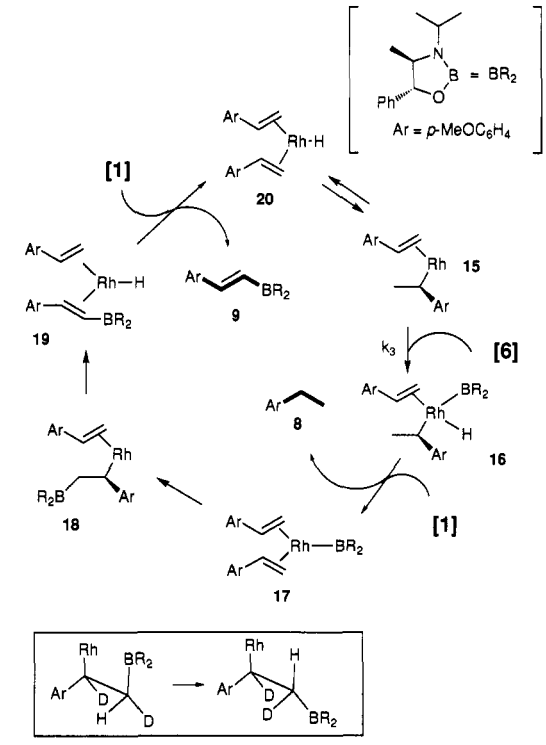

Figure 7. The catalytic cycle for formation of vinylborane **9** and alkane **8** from alkene **1** and oxazaborolidine **6**. Rate-limiting addition of B–H to rhodium leads to elimination of alkane and formation of Rh–boryl **17**. The vinylborane is then formed by β-migration of boron to coordinated alkene and β-elimination, which also regenerates the hydride **20**. The inset indicates the isotopic course of β-elimination with *syn* stereochemistry.

$Rh(PPh_3)_3$ with deuterated styrenes observed during studies of catalytic hydroformylation.[16]

Combining these observations on isotope exchange with the product analyses summarized in Figure 6 permits a mechanistic model to be made. The Rh-benzyl intermediate of Figure 5 is represented as structure **15** in Figure 7. This adds oxazaborolidine **6** to give complex **16**, followed by alkylhydride elimination, leading to alkane **8** and the rhodium boryl **17**. With a deuterated alkene the incoming hydride is then located completely at the benzylic site of the alkane, precluding pathways which permit isotope exchange between B–H and alkene **1**, and hinting that the borane addition step is rate-limiting. From **17**, the route to vinylborane **9** is indicated in Figure 7. This first requires β-boryl migration in **17** to give intermediate **18** and then β-hydride migration, which forms the alkene complex **19**. Migration of the boryl residue to the β-position must occur with complete regiospecificity giving **18**. There are analogies for this migration step in metal-silyls,[17] and recently Baker, Marder, and co-workers have provided a clear-cut example involving a rhodium boryl.[18] Exchange of vinylborane **9** for alkene **1** regenerates Rh hydride **20** and completes the catalytic cycle. In keeping with the likely instability of the Rh–H intermediates, the catalyst is only stable whilst the reaction is underway and rapidly becomes dark and heterogeneous on exhaustion of the reactants.

Consider α,β-dideuterated alkene ((*E*)-1,2-[^{2}H]$_2$)-**1**. Without the competing isotopic exchange processes, one atom of deuterium would be incorporated at both side-chain positions of the alkane and vinylborane products—given that the β-boryl migration and the β-hydride migration between **17** and **19** are *cis*-specific as indicated in the inset to Figure 7. As the scrambling and exchange processes are fast relative to borane addition, the alkene is equally distributed among α-d_1, *E*- and *Z*-d_2, and -d_3 isotopomers, ignoring equilibrium isotope effects. Analyzing the course of reaction for the d_2-isotopomer as a 50:50 *E*/*Z* mixture, the predicted deuterium atom distribution is then α: β 1:1.5 in the alkane product and α: β 1:0.5 in the vinylborane. For an equimolar mixture of α-d_1 and -d_3 alkene isotopomers, the same result is predicted, and an equipollent mixture of all four components in which all compete at both alkene processing stages would thus give this overall result. This closely, but not exactly, mimics the experimental results. Excess of deuterium over the predicted 0.5 atoms at C2 of **9** implies that borane addition is marginally competitive with isotope exchange. The small but real loss of deuterium from the 1-position of **9**, and the small difference between runs at different catalyst concentrations are less easily rationalized.

Reactions followed quantitatively by ^{1}H NMR are considered next. A set of experiments was carried out with the same batches of reagents on the same day. After addition of rhodium complex **7** a brief induction period (20–60 s) was consistently noted. The initial rate of consumption of oxazaborolidine **6** was determined by linear regression of the first three to five data points after the induction period. Although necessarily approximate, these results indicate that the reaction is half-order in rhodium complex **7**, is faster at higher concentrations of borane **6** and inhibited by higher concentrations of alkene **1**. This provides a model for the pre-rate-limiting portion of the catalytic cycle, shown in Figure 8. In this the active complex is the bisalkene rhodium hydride **20** for which the alternate reaction pathways are dimerization to **21**, alkene association to give **22**, and *cis*-β-hydride migration to give **15**. The latter process then leads into the catalytic cycle.

Based on the lack of isotope scrambling between B–H and the alkene a kinetic model was established in which the borane addition step **15** to **16** was rate-limiting for catalysis. The model requires fitting experimental data to two equilibrium constants K_1 (for alkene association wth hydride **20**) and K_2 (for dimer **21**

(16) Brown J. M.; Kent, A. G. *J. Chem. Soc., Perkin Trans 2* **1987**, 1597.
(17) Wakatsuki, Y.; Yamazaki, H.; Nakano M.; Yamamoto, Y. *J. Chem. Soc., Chem. Commun.* **1991**, 703.
(18) Baker, R. T.; Calabrese, J. C.; Westcott, S. A.; Nguyen, P.; Marder, T. B. *J. Am. Chem. Soc.* **1993**, *115*, 4367–8.

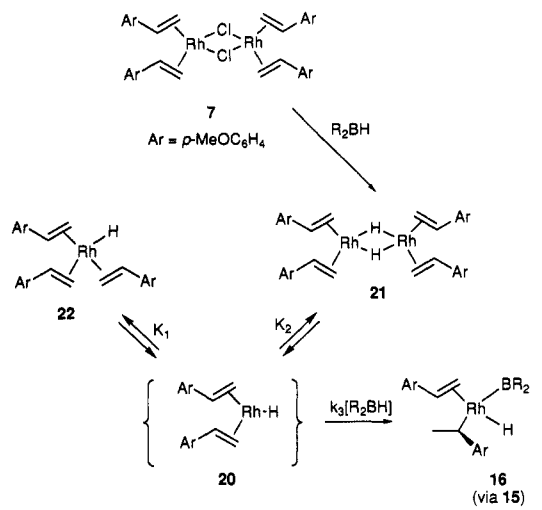

Figure 8. Initial phases of the catalytic cycle for reaction of alkene **1** with catalyst precursor **7**, demonstrating the reduction to a dimeric hydride **21**, its dissociation to monomer **20**, and the association of alkene giving **22**.

dissociation) and a bimolecular rate constant k_3 for the borane addition stage, assuming that the subsequent steps are fast. The values are interdependent and cannot be separately evaluated, but if the hypotheses are correct, then a single set of rate and equilibrium constants will be capable of simulating all the experimental data. Modeling was carried out using the GEAR routines transcribed for operation on a PC.[19] Two *formal* fast steps were included to complete the catalytic cycle, the first $k_4 = 1.0 \times 10^3$ s^{-1} to link intermediates **16** and **18**, and the second $k_5 = 1.0 \times 10^5$ mol^{-2} dm^6 s^{-1} to release vinylborane **9** and add two alkenes to reestablish the Rh hydride **20**; the model is not sensitive to these steps. Single or logically linked sets of the remaining rate or equilibrium constants K_1, K_2, and k_3, were adjusted iteratively. When $K_1 = 7.96 \times 10^{-6}$ mol dm^{-3}, $K_2 = 3.6 \times 10^{-2}$ mol dm^{-3}, and $k_3 = 16.8 \pm 2.5$ mol^{-1} dm^3 s^{-1}, the model fitted the full series within experimental error as shown in Figure 9. The results support the veracity of the proposed mechanism because of the close correspondence between experimental and enumerated data, over a range of concentrations of catalyst, reagent, and alkene which generate quite distinct time evolution curves. Closer examination of Figure 9 shows the relevant trends. In entries 1–3 the rhodium concentration is increased monotonically, and the reaction time decreases accordingly. Entry 4 is similar to entry 2 save that the concentration of borane **6** is higher thus increasing the observed rate. In entry 5 the alkene concentration is increased relative to entry 2, and the reaction is visibly slowed.

Vinylboranes from Catecholborane. Several authors have studied the Rh–complex catalyzed addition of catecholborane (**HBCat**) to vinylarenes,[2,4,7,12,20,21] and it is now known that if Wilkinson's catalyst is used the regiochemistry depends on the quality of the complex. Commercial $ClRh(PPh_3)_3$ may contain both peroxides[22] and Rh(II) impurities[23] which are absent from freshly prepared samples made from the corresponding cyclooctene complex.[24] Evans and co-workers[7] reported essentially complete formation of the secondary borane when styrene is employed. Furthermore, the deuterium from **DBcat** is located entirely at the methyl carbon of the product, and there is no concurrent H–D exchange in the reacting alkene. This regiochemistry is in accord with earlier observations of Mannig and Nöth[2] but contrasts with results of Hayashi and co-workers[4] and also with the earlier work of Burgess and co-workers[21] who reported that a major product in the addition to styrene is the primary borane (deuterated comparably at both sites) and that the reacting alkene undergoes substantial H–D exchange. The discrepancy was attributed by Evans and co-workers[7] to the purity of the catalyst, and this view is now accepted by Burgess and co-workers who report an extensive analysis of the effect of the catalyst history on the regioselectivity.[12] Both groups were able to lower the regioselectivity of styrene hydroboration by preexposing their catalyst to oxygen, the extent of primary product increasing with the degree of exposure. The phenomenon was countered by adding excess PPh_3, although the mechanism of the oxygen effect was not discussed in detail. A tentative suggestion to explain part of the pathway would be that oxidation produces a phosphine-poor complex which encourages the formation of vinylborane in a similar manner to the chemistry described for oxazaborolidine **6**. Previous authors had not reported β-arylvinylboranes in the vinylarene reaction, but that could be attributed either to their adventitious hydrogenation (which requires some disproportionation of the reagent with generation of H_2),[12,24] to primary borane or to their loss as the corresponding carboxylic acid in a basic oxidative workup procedure.

To probe this further, experiments were carried out in which alkene **1** was subjected to hydroboration catalyzed by complex **7** with different boranes. With the simple oxazaborolidine derivatives from ephedrine and φ-ephedrine, rapid reaction ensued to give the alkane **8** and the corresponding vinylborane in equal amounts. In contrast to borane **6**, a detectable amount of the primary borane (≤2%) was observed, but the secondary borane was absent. When **HBcat** was used, the reaction was extremely rapid, corresponding to several hundred turnovers of catalyst per minute. During turnover the solution was bright yellow, becoming brown immediately the reagents were expended. When the reaction was carried out in C_7D_8 solution and immediately analysed by ^{1}H NMR, three products were observed in comparable amounts, these being the alkane **8** and vinylborane **23** together with the primary borane **24**. Secondary borane, the dominant product of phosphine-complex catalyzed hydroboration, was not detected.

The mechanism of alkane and vinylborane formation could be similar to that already delineated above for oxazaborolidine **6**, but the concurrent formation of some primary borane **24** together with complete absence of secondary borane is not yet explained. Given the high reactivity of **HBcat** in its addition to square-planar rhodium complexes it suggests that compound **24** could be formed by an extension of the catalytic cycle discussed above, as indicated in Figure 10. In this modification the intermediate **27** (corresponding to **18**) undergoes a competitive second-order reaction with a further molecule of **HBcat**. The adduct **26** then produces primary borane **24** by reductive elimination and regenerates the rhodium boryl **25**. Depending on the relative efficiency of the first- and second-order competing pathways, this mechanism gives predominantly vinylborane or primary borane; indeed if the **HBcat** addition were sufficiently rapid then primary borane **24** would be formed exclusively. The proposal

(19) GIT-GEAR numerical integration routine (PC-version): Weigert, F. J. *Computers and Chemistry* **1987**, *11*, 273. Stabler R. N.; Cheswick, J. *Int. J. Kinet.* **1978**, *10*, 461. McKinney R. J.; Weigert, F. J. Quantum Chemistry Program Exchange, program No. QCMPO22. A copy from Dr. R. J. McKinney (Dupont) is gratefully acknowledged. The program was used in two distinct ways. For the results displayed in Figure 9, sets of experimental data were subjected to the iterative procedure (GIT) until the quality of nonlinear least-squares fit could not be further improved. For the results displayed in Figure 11 GEAR simulations employing experimental initial concentrations were run to completion according to the model of Figure 10, with k_6 fixed and k_7 varied until the final concentrations of the primary borane product **24** fitted over the range of initial conditions. The same value of k_7 was used to produce the remaining plots. A similar approach, where k_{10} was kept constant and k_{11} varied, was used to produce Figure 14.

(20) Zhang, J.; Lou, B.; Guo G.; Dai, L. *J. Org. Chem.* **1991**, *56*, 1670.

(21) Burgess, K.; van der Donk, W. A.; Kook, A. M. *J. Org. Chem.* **1991**, *56*, 2949.

(22) Carvalho, M.; Weiserman, L. F.; Hercules, D. M. *Appl. Spectrosc.* **1982**, *36*, 290.

(23) Ogle, C. A.; Hubbard, J. C.; Masterman, J. L. *J. Chem. Soc., Chem. Commun.* **1991**, 1733.

(24) Noshiguchi, T.; Tachi, K.; Fukuzami, K. *J. Org. Chem.* **1975**, *40*, 240.

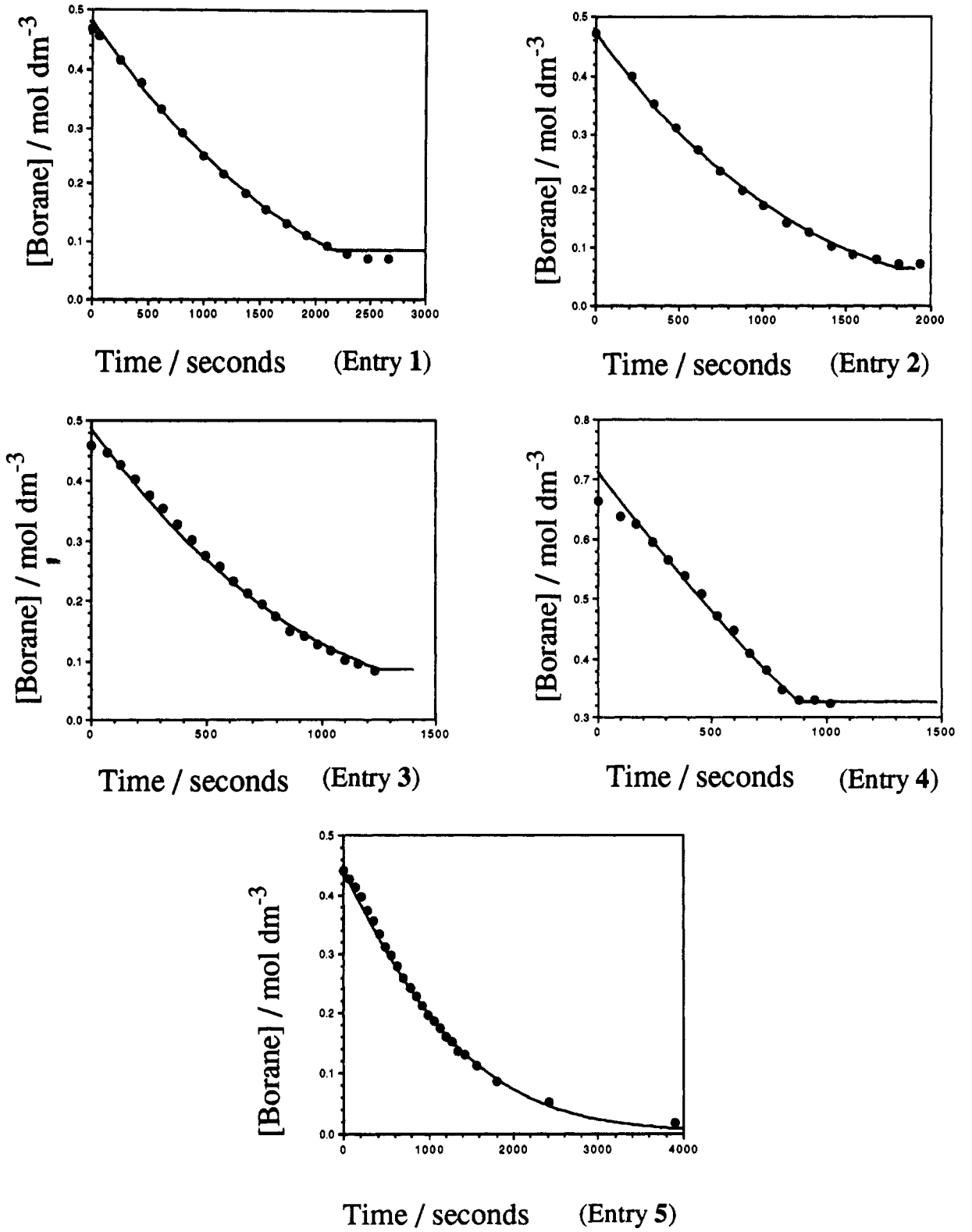

Figure 9. Experimental data (solid circles) and GEAR simulations (continuous lines) according to the model of Figures 7 and 8 for a series of reactions of alkene **1** with oxazaborolidine **6** catalyzed by complex **7** in C_7D_8 at 25 °C—rate constants for simulations as text; concentrations of **1**, **6**, and **7**, respectively, follow: entry 1 0.46 M, 0.75 M, 0.18 mM; entry 2 0.46 M, 0.75 M, 0.36 mM; entry 3 0.46 M, 0.75 M, 0.54 mM; entry 4 0.66 M, 0.71 M, 0.35 mM; entry 5 0.44 M, 1.06 M, 0.35 mM.

carries a specific prediction, tested by simulation procedures, that the proportions of these two products will depend on the initial concentration of **HBcat**.

A series of experiments were carried out in C_7D_8 in which the final concentration of alkene, alkane, primary borane, and vinylborane were measured by ^1H NMR integration of their side-chain resonances. It was discovered that if there was a delay of ≥2 h before the measurement was made, then the proportion of vinylborane (relative to alkane) decreased measurably and the proportion of primary borane increased concomitantly. For a series of samples left for 12 h before analysis, it was found that the excess of primary borane increased linearly with the initial [Rh] catalyst concentration. Hence the residual catalyst is capable of hydrogenating the vinylborane product with H_2 produced by excess catecholborane disproportion[12,24] and care was taken in subsequent runs described below to analyze the

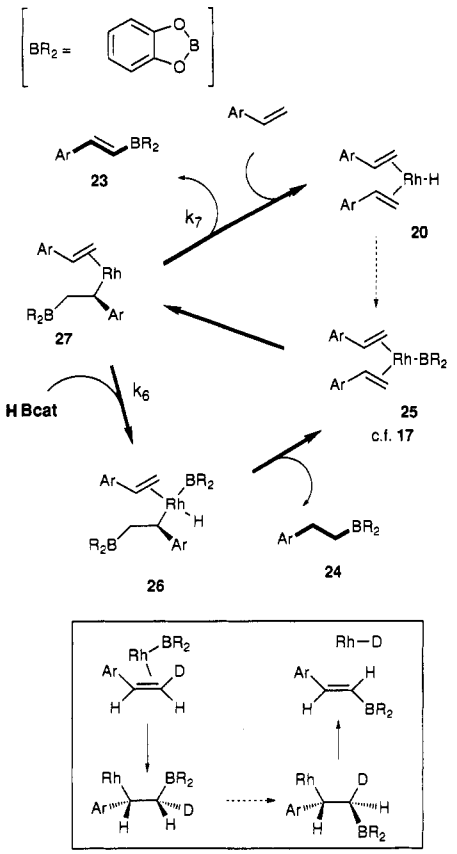

Figure 10. The secondary catalytic cycle in reaction of alkene **1** with **HBcat** catalyzed by complex **7**, leading from a common intermediate **27** to the formation of primary borane **24** in a second-order step which competes with the first-order step of the main cycle which leads to vinylborane **23**. The path from **20** to **25** is identical to the route from **20** to **17** in Figure 7. The inset indicates how a stereospecific addition–elimination sequence leads on to undeuterated vinylborane **23** from (*Z*)-2-monodeuterated alkene.

product mixtures as soon as practicable after the catalytic reaction was over, observing the characteristic color change from orange to brown. In such runs the yields of alkane **8** and vinylborane **23** were identical. In experiments with 1,2,2-trideuterated alkene **1** and **HBcat** the primary borane product **24** was trideuterated within experimental error, showing that none came from adventitious hydrogenation of vinylborane **23** with H_2 from **HBcat** decomposition. The product distribution was very different when ((*Z*)-2-[^{2}H])-**1** or (1,2,2-[^{2}H]$_3$)-**1** were employed when compared to unlabeled **1**, with a lower proportion of undeuterated or 1,2-[^{2}H]$_2$ vinylborane **23**, respectively, formed (by ^{1}H NMR), and 1,2-dideuterated alkane **8** in the former case. When ((*E*)-1,2-[^{2}H]$_2$)-**1** was employed, the deuterium was retained in both products **24** and **23**, whose ratio was similar to that observed in the undeuterated case. This shows that there is a primary isotope effect militating against vinylborane formation when D rather than H is involved in the β-hydride elimination step, inset in Figure 10. When **DBcat** was employed, the product ratios were close to those obtained with the undeuterated reagent, implying the lack of a primary isotope effect on the competition between first- and second-order pathways from **27**.

The indicated pathway can be tested by running GEAR models and comparing the predicted and observed product proportions at completion. For the catalytic cycle shown in Figure 10, rate constants other than k_7 were assigned values, and k_7 was varied iteratively for a single set of initial concentrations until the predicted value accorded with experiment. It then proved possible to obtain a good fit of the final concentration of **24** for five other experiments with this same value of k_7 (Figure 11a). Moreover, this same value successfully predicted the final concentration of both alkane **8** and vinylborane **23** and that of residual alkene **1** for the complete set (Figure 11b–d). These plots were obtained with a value for k_7 of 10 s^{-1}, holding k_6 at 30 mol^{-1} dm^3 s^{-1} so that the ratio of the two competing rate constants k_6/k_7 was 3.0 mol^{-1} dm^3. The best fit for two runs with trideuterated alkene was obtained when k_7 = 2.95 s^{-1} and here k_6/k_7 = 10.2 mol^{-1} dm^3. This corresponds to a primary isotope effect for the β-elimination step of 3.4; comparable with typical literature values.[26]

As expected, the proportion of primary borane (favored by the second-order process) increased with decreasing temperature, although it was never more than 65% of the total borane product even at −50 °C. Key differences were noted between hydroboration with **HBcat** and with borane **6**. The former is much more reactive and adds rapidly to Rh benzyl **15** since none of the isotope scrambling processes discussed earlier are observed; the kinetic isotope effect depends on the isotopic integrity of intermediates in the cycle. In principle, the respective roles of the two molecules of **HBcat** involved in the catalytic cycle of Figure 10 can be further delineated by a double labeling experiment, since the mechanism suggests that the B and H of catecholborane are delivered to different molecules of alkene and hence appear in separate molecules of primary borane **24**. To test the feasibility catecholborane-d_5 was prepared from catechol-d_4 and BD_3.[27] It was confirmed by GC/MS analysis that it was of high isotopic purity. Direct analysis of a mixture of d_5- and d_0-catecholborane instantly after mixing and injection (C_7D_8 solution, direct injection into the ion source) indicated that isotopic exchange was essentially complete because the deuterium was randomized between d_0, d_1, d_4, and d_5 isotopomers. Although catecholborane is monomeric in solution, the reversible dimerization is rapid-exchange occurring to completion on a time scale of 10–10^2 s, precluding the desired double-labeling experiment.

The Mechanism of Rhodium-Catalyzed Silation. The observation of competing additive and desaturative hydroboration described here is reminiscent of observations made in the course of catalyzed hydrosilylations, in which the formation of vinylsilanes is a well-known side reaction. For example, $Ru_3(CO)_{12}$ promotes near-quantitative formation of vinylsilanes (based on Si) from the reaction of $HSiEt_3$ with a range of vinylarenes.[28] The effect of added oxygen gas has been noted in hydrosilylations catalyzed by [$RhCl(PPh_3)_3$][29,30] and also by other rhodium phosphine complexes.[31] The hydrosilylation of hex-1-ene catalyzed by [$RhCl(PPh_3)_3$], in which vinylsilane products were observed, required O_2 to initiate catalysis. It was suggested that the oxygen removed some or all of the phosphine ligand by oxidation. The reactions displayed an induction period and were found to be half-order in rhodium. Furthermore, the reacting solution gave no observable ESR signal and reaction could not be triggered by addition of radical initiators or the rate retarded by the addition of radical traps. Similar results were obtained with a range of iridium complexes.[32] Vinylsilanes were observed as side products

(25) Westcott, S. A.; Taylor, N. J.; Marder, T. B.; Baker, R. T.; Jones, N. J.; Calabrese, J. C. *J. Chem. Soc., Chem. Commun.* **1991,** 304. Westcott, S. A.; Blom, H. P.; Marder, T. B.; Baker, R. T.; Calabrese, J. C. *Inorg. Chem.* **1993,** *32,* 2175.

(26) Zamashchikov, V. V.; Mitchenko, S. A.; Shubin, A. A.; Kostenko, E. L. *Kinetics and Catalysis* **1992,** *33,* 400–3. Cross, R. J. *Chemistry of the Metal-Carbon Bond*; Hartley, F. R.; Patai, S., Eds.; John Wiley and Sons: New York, 1985. McDade, C.; Green, J. C.; Bercaw, J. E. *Organometallics* **1982,** *1,* 1629. Ikariya, T.; Yamamoto, A. *J. Organomet. Chem.* **1976,** *120,* 257.

(27) Baban, J. A.; Goodchild, N. J.; Roberts, B. P. *J. Chem. Soc., Perkin Trans. II* **1986,** 157.

(28) Seki, Y.;Takeshita K.; Kawamoto, K.; Murai, S.; Somada, N. *Angew. Chem., Int. Ed. Engl.* **1980,** *19,* 928.

(29) Dickers, H. M.; Haszeldine, R. N.; Malkin, L. S.; Mather A. P.; Parish, R. V. *J. Chem. Soc., Dalton Trans.* **1980,** 308.

(30) de Charentanay, F.; Osborn J. A.; Wilkinson, G. *J. Chem. Soc. A* **1968,** 787.

(31) Millan, A.; Fernandez, M.-J.; Bentz, P.; Maitlis, P. M. *J. Mol. Catal.* **1984,** *26,* 89.

(32) Oro, L. A.; Fernandez, M. J.; Esteruelas, M. A.; Jimenez, M. S. *J. Mol. Catal.* **1986,** *37,* 151.

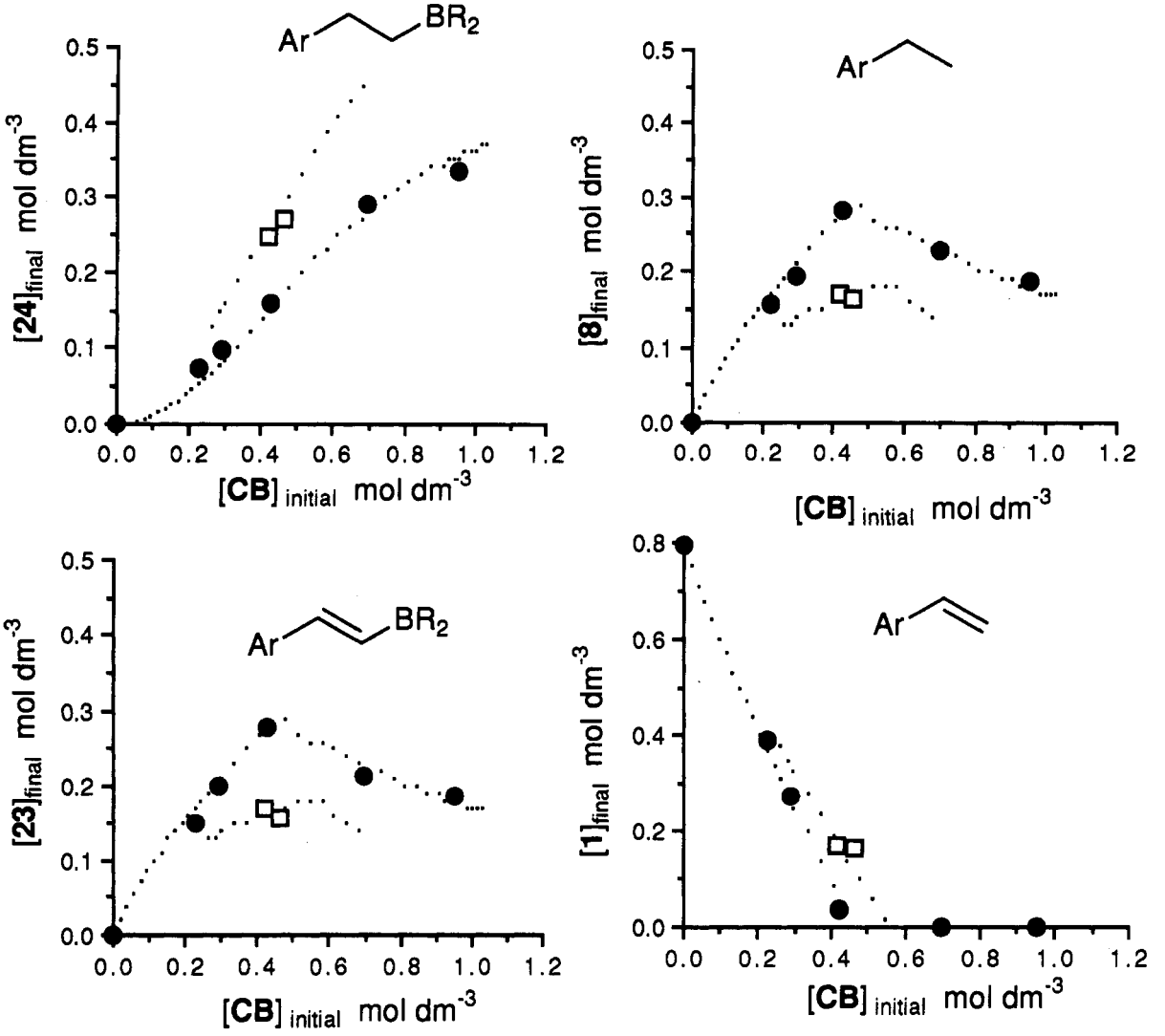

Figure 11. Filled circles: The final product and residual reactant proportions observed for a series of catalytic reactions in C_7D_8 at 20 °C, initial concentrations of **HBcat** as X-axis, of alkene **1** (0.74 ± 0.03 M) and of catalyst precursor **7** (0.77 mM, save 1.42 mM in run 5). The dotted lines represent the predicted product proportions derived from a GEAR model based on the competing paths shown in Figure 10 and employing the rate constants indicated in the text. Open squares: as above but employing (1,2,2-[^{2}H]$_3$)-**1** (0.75 M) and comparing with predictions which incorporate a kinetic isotope effect for the β-elimination step of 3.4.

during the hydrosilylation of phenylethene catalyzed by [RhCl(PPh$_3$)$_3$]. Induction periods of up to 30 min were observed. [RhH(CO)(PPh$_3$)$_3$] was found to be more selective than [RhCl(PPh$_3$)$_3$] toward vinylsilane formation.[33] Significantly, both of the reactions were completely inhibited by addition of PPh$_3$. The suggestion was made, by a referee of that manuscript, that substitution of the PPh$_3$ ligands on [RhCl(PPh$_3$)$_3$] by the alkene substrate may play an important part in the catalytic cycle.[34] Vinylsilane intermediates were inferred to account for product deuterium label distributions during a recent mechanistic investigation[35] of intramolecular asymmetric hydrosilylation of alkenes.[36]

The mechanism of silation (vinylsilane formation) under hydrosilylation conditions has been discussed widely, with some authors suggesting variants on the original catalytic cycle proposed by Chalk and Harrod.[37] This is illustrated schematically in Figure 12, with **A** and **B** the normal and variant pathways, respectively, starting with a metal complex M. Silation by this mechanism requires that β-hydride migration competes successfully with reductive elimination of silane. For other cases an alternative has been suggested, first by Wrighton and co-workers, which involves a catalytic complex M–H interconverting with M–SiR$_3$ as indicated in Figure 12C. This is exemplified by a detailed study of Cp*(CO)$_2$Fe(SiMe$_3$) and its derivatives as photoactivated hydrosilylation catalysts. In stoichiometric experiments, the thermal insertion of ethene into the Fe–Si bond to afford Cp*(CO)$_2$FeCH$_2$CH$_2$SiMe$_3$ was observed. Subsequent photolysis of this yielded vinyltrimethylsilane via a β-H elimination.[38] In the catalytic mechanism, the silylmetal intermediate formed by addition/elimination can effect a β-elimination to give vinylsilane or act as a conduit for the formation of alkylsilane through the successive addition of alkene and R$_3$SiH as shown. Modifications of this postulate have also been suggested by Perutz, Maitlis, and their respective co-workers.[39]

In preliminary experiments it was demonstrated that hydrosilylation of alkene **1** with HSiEt$_3$ catalyzed by the corresponding complex **7** resembled the hydroborations discussed above. In particular, the product was a mixture of (*E*)-vinylsilane **28** and

(33) Onopchenko, A.; Sabourin, E. T.; Beach, D. L. *J. Org. Chem.* **1983**, *48*, 5101.
(34) Onopchenko, A.; Sabourin, E. T.; Beach, D. L. *J. Org. Chem.* **1984**, *49*, 3389.
(35) Bergens, S. H.; Noheda, P.; Whelan, J.; Bosnich, B. *J. Am. Chem. Soc.* **1992**, *114*, 2128.
(36) Tamao, K.; Toma, T.; Inui, N.; Nakayama O.; Ito, Y. *Tetrahedron Lett.* **1990**, *31*, 7333. Bergens, S. H.; Noheda, P.; Whelan, J.; Bosnich, B. *J. Am. Chem. Soc.* **1992**, *114*, 2121.
(37) Chalk, A. J. ; Harrod, J. F. *J. Am. Chem. Soc.* **1965**, *87*, 16 .
(38) Randolph C. L.; Wrighton, M. S. *J. Am. Chem. Soc.* **1986**, *108*, 3366. Seitz, F.; Wrighton, M. S. *Angew. Chem., Int. Ed. Engl.* **1988**, *27*, 289.
(39) Duckett , S. B.; Perutz, R. N. *Organometallics* **1992**, *11*, 90. Millan, A.; Fernandez, M. J.; Bentz, P.; Maitlis, P. M. *J. Mol. Catal.* **1984**, *26*, 89.

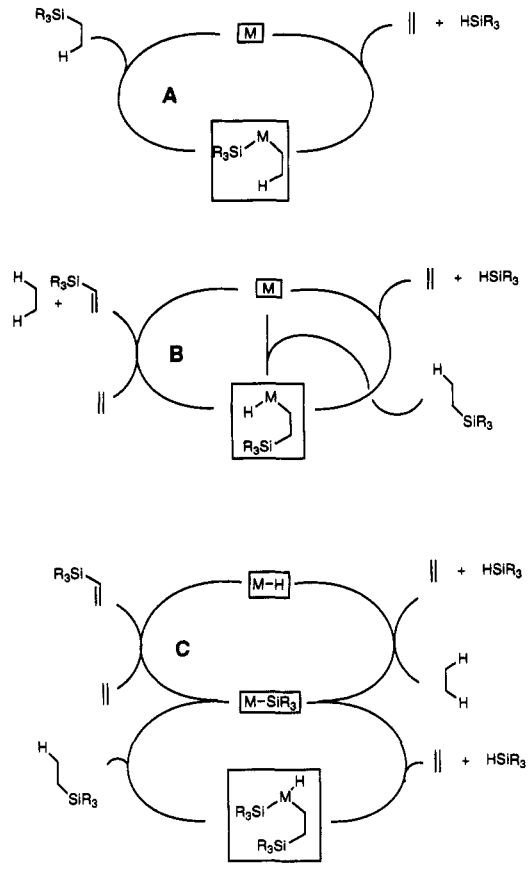

Figure 12. Variations on the original Chalk–Harrod hydrosilylation mechanism which lead to competitive silation: (A) original mechanism of Chalk and Harrod; (B) Pathway involving silyl migration which permits competing silation; and (C) metal hydride catalyst with the dual competing pathways.

alkane **8** in equivalent proportions together with some *primary* hydrosilylation product **29**. Except at high initial concentrations of the silane the secondary hydrosilylation product 1-(4-methoxyphenyl)triethylsilylethane **30** is not formed in significant amount. Using deuterated analogs of alkene **1** as before, the product proportions were different. Under comparable conditions (room temperature, 0.2 mol% **7**, C_6D_6, 10–20 h) ((*E*)-1,2-[^{2}H]$_2$)-**1** gave rise to 40% of primary silane **29** whilst the undeuterated alkene gave 27%; the remainder of the product in both cases being equipartitioned between alkane **1** and vinylsilane **28**. Generally speaking, the catalytic turnover is quite slow and reactions were left for 12–24 h to ensure completion. In control experiments it was also ascertained that catalytic turnover under these conditions was accompanied by *E*–*Z* isomerization of ((*E*)-1,2-[^{2}H]$_2$)-**1** and by exchange between $HSiEt_3$ and (1,2,2-[^{2}H]$_3$)-**1**. Rapid equilibration of isotopic label between $HSiMe_2Ph$ and $DSiEt_3$ was also observed under the conditions of catalysis, in the presence of complex **7**. Hence the hydrosilylation exhibits very similar characteristics to hydroboration with **HBcat** catalyzed by the same complex; the product distribution is affected by isotopic substitution at the 2-position (although the detailed interpretation is complicated by competing exchange and isomerisation), and the catalyst behaves as if it were a rhodium hydride.

The critical part of the silation mechanism of Figure 12C adapted to the present reaction system is shown in Figure 13, closely resembling the pathway for catalytic hydroboration and boration with **HBcat** suggested earlier. Since this mechanism is in accord with the isotopic labeling studies in our $HSiEt_3$ additions, further work was carried out. Proceeding as before, the final proportions of primary silane **29** and vinylsilane **28** were measured in a series of catalytic reactions for which the initial silane concentration was systematically varied. In all cases the yields

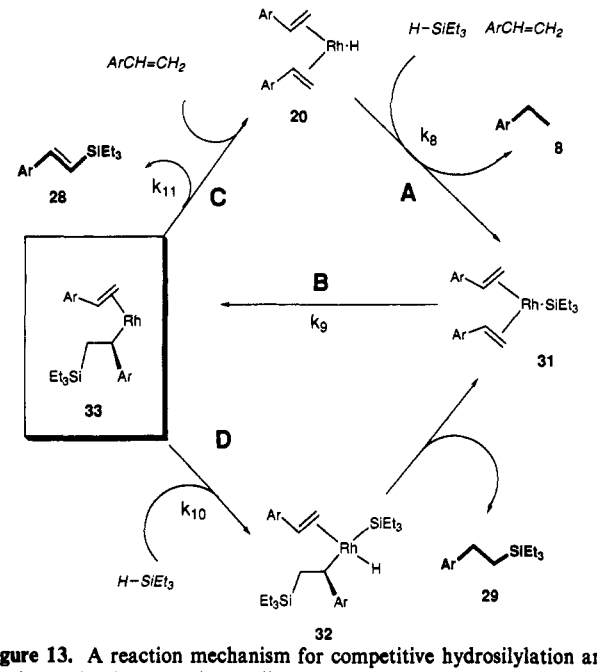

Figure 13. A reaction mechanism for competitive hydrosilylation and silation which involves the rhodium hydride **20** and the corresponding rhodium silyl **31**. The vinylsilane **28** is produced by a first-order β-elimination in **33** and the primary silane **29** by second-order $HSiEt_3$ addition to the same intermediate.

of vinylsilane **28** and alkane **8** were identical within experimental error. The results were compared with the predictions of a GEAR model in which rate constants k_8, k_9 and k_{10} were assigned values of 1×10^4 mol^{-2} dm^6 s^{-1}, 1×10^4 s^{-1}, and 7.0 mol^{-1} dm^3 s^{-1}, respectively—the first two are set to be fast, and k_{10} to be rate-limiting at approximately the observed rate of turnover. Rate constant k_{11} was then varied in steps; under these conditions the product distribution is determined solely by the relative values of k_{10} and k_{11}. With a value for k_{11} of 1.0 s^{-1} and hence a ratio k_{10}/k_{11} of 7.0 mol^{-1} dm^3, the predicted final distributions (including reactant) fit with the data (Figure 14) to within experimental error. This leads to the conclusion that the vinylsilane and primary silane are produced in competing first- and second-order paths from a common intermediate **33**. This can either add $HSiEt_3$ giving **32** which then eliminates primary silane **29** and reverts to the silylrhodium complex **31** and hence back to **33** [path **B** → **D**, Figure 13]; alternatively, the latter intermediate **33** can undergo β-elimination directly to give the vinylsilane **28** and reenter the main catalytic cycle *via* rhodium hydride **20** [Path **B** → **C**, Figure 13].

For conventional hydrosilylations with Rh phosphine catalysts, the "oxygen effect" causing acceleration is probably due to the formation of species related to **20**, which can catalyze the formation of primary silanes from vinylarenes. Other features of silation with Rh catalysts—e.g., the enhanced formation of unsaturated silanes at high dilution of catalyst,[33] indicate a likely role for phosphine-free or phosphine-poor catalysts and a Rh-hydride mediated catalytic cycle.

Summary and Conclusions

This work originated with the observation that catalytic hydroboration of alkenes using oxazaborolidine **6** was substantially slower than with the analogous reagent **2** and gave the alkane **8** and vinylborane **9** as major products. It was discovered that the true catalyst for this path was derived by decomposition of the diphosphine rhodium precursor to a phosphine-free complex, and a rapid quantitative reaction was observed when the alkene complex **7** was employed as catalyst. This reaction was shown by deuterium-labeling experiments and by analysis of the reaction kinetics to involve a monomeric rhodium hydride catalyst. The

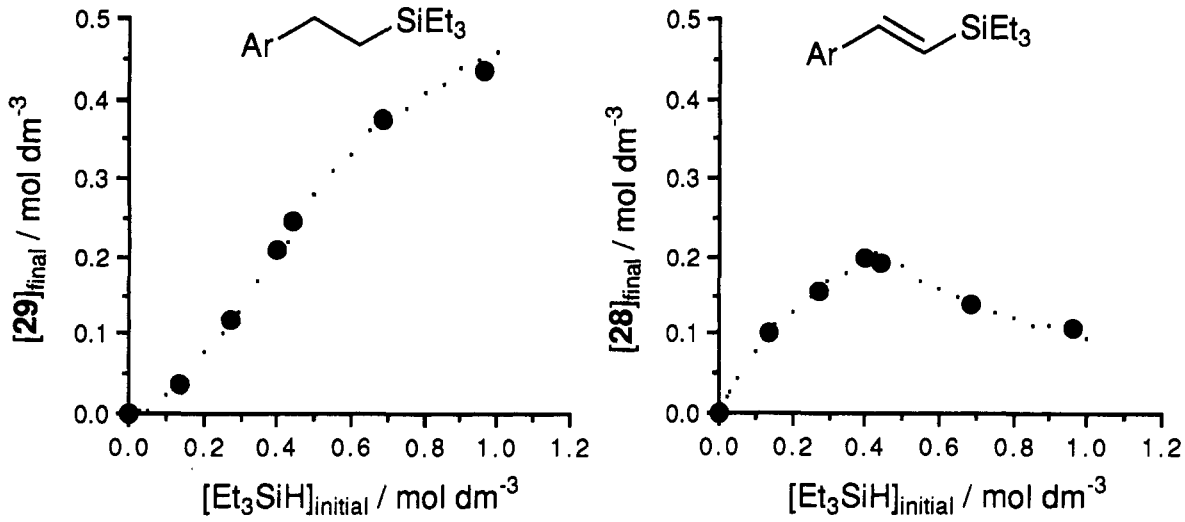

Figure 14. Proportions of vinylsilane **28** and primary silane **29** formed in the hydrosilylation of alkene **1** (0.65 M) with $HSiEt_3$ (initial concentration as X-axis) catalyzed by complex **7** (0.0033 M) in C_6D_6 at 20 °C. Analysis was carried out by ^1H NMR at 500 MHz after 18 h. The dotted lines represent the predictions of the model using the rates constants described in the text and following the same protocol as for Figure 11.

model described by Figures 7 and 8 was developed and shown to simulate the observed reaction kinetics well.

When the same catalyst is used with **HBcat** as the addend, the primary borane **24** is produced in varying amounts, in addition to the vinylborane and alkane products. The product ratios could be accurately simulated by assuming that a late intermediate in the catalytic cycle (**27** in Figure 10) adds **HBcat** in competition to the β-hydrogen elimination step to give **26**, effectively short-circuiting the cycle. The veracity of this suggestion was tested by examining the product ratios as a function of initial [**HBcat**], since the ratio of **23** to **24** is determined by competing first- and second-order steps. A good fit of the data was obtained when the ratio of these, k_6/k_7, was 3.0 mol^{-1} dm^3. When the alkene was isotopically labeled, the ratio giving best fit was k_6/k_7 = 10.2 mol^{-1} dm^3 and this can be rationalized if the β-elimination step is associated with a kinetic isotope effect of 3.4.

The desaturative boration process observed here resembles Rh-catalyzed silation, which has been observed and discussed regularly. It was found that the pathway proposed for **HBcat** catalyzed reaction applied equally well to the $HSiEt_3$ reaction with the same catalyst **7**, and the relative proportions of primary silane **29** and vinylsilane **28** were simulated by a similar model, with k_{10}/k_{11} = 7.0 mol^{-1} dm^3.

Given the range of opportunities presented by the multistep cycles involved, the catalytic reactions are extremely clean. This gives an insight into the relative rates of potential competing processes. Rhodium hydride **20**, which is the key to all the reactions described, must be very labile. This is the likely reason why the observed chemistry is confined to vinylarenes, which bind strongly to rhodium; presumably simple alkenes cannot prevent rapid reduction to the metallic state because they dissociate too readily. The cis β-ligand migration of hydride (**20–15**) and of boryl or silyl (**17–18**; **25–27**; **31–33**) always occurs with complete regiospecificity to give the Rh–benzyl complex. Although this is likely to be the more stable of the two alkyl intermediates, the specificity seems considerably higher than in, e.g., hydroformylation of vinylarenes[40] so that the specific participation of the arene in α,1,2-η^3-coordination has to be considered. Examples involving such bonding in coordinatively unsaturated complexes are well-known.[41] The Rh(III) complexes **16** and **26** preferentially eliminate C–H rather than C–B, and a similar conclusion applies to intermediate **32**; disilanes are not detected. There is a strong implication that the "conventional" mechanism for catalytic hydroboration with Rh–phosphine complexes does not involve either a hydride-free Rh boryl (cf. **17**) or a boryl-free Rh hydride (cf. **20**) else the vinylborane route would be more prevalent. The observed α-delivery of the boryl group in catalytic hydroboration of vinylarenes with PPh_3 or catenated diarylphosphines[7,12] implies that hydride transfer occurs first to give the Rh–benzyl and that C–B reductive elimination occurs subsequently. There needs to be caution about generalization because Rh–isopropylphosphine complexes have been shown by Marder, Baker, and co-workers to produce an excess of the primary arylethylborane-derived alcohol after oxidative workup.[7]

Taken together, the results emphasize the distinct catalytic chemistry of "bare" rhodium hydrides, which are highly reactive relative to phosphine complexes. The observations may provide assistance in explaining the shift from secondary to primary borane formation when part-oxidized Wilkinson's catalyst is used in the catalytic hydroboration of styrenes, although that reaction is clearly different in some respects[42] (e.g., the lack of isotopic scrambling between **DBcat** and styrene observed here, in contrast to that described for the oxidized $ClRh(PPh_3)_3$ case). The synthetic utility is at present confined to the direct formation of (*E*)-β-arylvinylboranes and (*E*)-β-arylvinylboronic acids from arylalkenes. Extensions to related reactions involving activation of boranes and their derivatives is in train.

Experimental Section

General Methods. Elemental microanalyses were carried out by Mrs V. Lambourn in the Dyson Perrins Laboratory, using a Carlo Erba 1106 elemental analyzer. ^1H NMR spectra were recorded on Varian Gemini

(40) For η^3-benzylrhodium complexes, see: Stuhler, H.-O.; Pickardt, D. T. Z. *Naturforsch, B* **1981**, *36*, 315. Chappell, S. D.; Cole-Hamilton, D. J.; Galas, A. M. R.; Hursthouse, M. B.; Walker, N. P. C. *Polyhedron* **1985**, *4*, 121. Ebbinghaus, B.; Madigan, T. J.; Osterberg, C. E.; Nathan, L. C. *Acta. Crystallogr. C* **1988**, *44*, 21.

(41) For recent examples, see: Jongsma, T.; Challa, G.; van Leeuwen, P. W. N. M. *J. Organomet. Chem.* **1991**, *421*, 121. Oswald, A. A.; Hendriksen, D. E.; Kastrup, R. V.; Moseleski, E. J. *Adv. Chem. Ser.* **1992**, *230*, 395. Kwok, T. J.; Wink, D. J. *Organometallics* **1993**, *5*, 1954 and refs therein.

(42) A number of species which may influence the course of hydroboration are present in part-oxidized $ClRh(PPh_3)_3$, including dioxygen complexes and PPh_3O, making direct analogy with the present work difficult. When the reaction of styrene and **HBCat** was carried out in C_7D_8 using a solution of $ClRh(PPh_3)_3$ which had been standing in air, some vinylborane, but no ethylbenzene, was observed in the NMR spectrum of crude product. We thank Dr. T. P. Layzell for this experiment.

(43) Perrin, D. D.; Armarego, W. L. F. *Purification of Laboratory Chemicals*, 3rd ed.; Pergamon Press: 1988.

(44) Allen, A. D.; Cook C. D. *Can. J. Chem.* **1963**, *41*, 1084. Trumbull, E. R.; Finn, R. T.; Ibne-Rasa, K. N.; Sauers, C. K. *J. Org. Chem.* **1965**, *27*, 2339.

200 (200 MHz), Bruker AM 250 (250 MHz), Bruker WH 300 (300 MHz), or Bruker AM 500 (500 MHz) spectrometers. ^{2}H NMR spectra were recorded on a Bruker AM 500 (76.774 MHz) and are referenced to solvent ($CDCl_3$ δ = 7.27); (C_6D_6 δ = 7.16) and (C_7D_8 δ = 2.09). ^{13}C NMR spectra were recorded on Varian Gemini 200 (50.31 MHz), Bruker AM 250 (62.89 MHz), or Bruker AM 500 (125.8 MHz) spectrometers.^{11}B NMR spectra were recorded on a Bruker AM 250 (80.21 MHz) spectrometer and are externally referenced to $BF_3{\cdot}Et_2O$ ($\delta 11_B$ = 0.0). ^{29}Si NMR spectra were recorded on a Bruker AM 250 (49.69 MHz) ref $SiMe_4$ ($\delta 29_{Si}$ = 0.0). ^{1}H NMR kinetics experiments were performed on a Bruker AM 500 spectrometer. IR spectra were recorded on a Perkin Elmer 1750 fourier transform spectrometer. Mass spectra were recorded on a Trio-1 GCMS (Hewlett Packard GC) spectrometer or on a VG 20–250 spectrometer. Optical rotations were recorded on a thermostatted Perkin-Elmer 241 polarimeter, using the 589.3 nm Na D-line. Samples were prepared under argon as solutions in spectrophotometric grade $CHCl_3$. Melting points were recorded on a Reichert–Koffler block and are uncorrected. All manipulations of oxygen or water sensitive materials were carried out under argon using standard vacuum line and Schlenk techniques. All alkenes (from CaH_2), boranes, and silanes were distilled under argon or vacuum immediately before use. Solvents were purchased from Rhône-Poulenc, Fisons, May & Baker, or the Aldrich Chemical company and were dried before use according to the procedures described by Perrin and Armarego.[43] Deuterated solvents and reagents were purchased from the Aldrich Chemical company or from Sigma. D_2SO_4 and D_2O were stored in ampoules, under argon. $CDCl_3$ was either dried over 4 Å molecular sieves or distilled from P_2O_5 immediately before use. C_6D_6 and C_7D_8 were stored over, and then distilled from, CaH_2 under argon immediately before use.

1*R*,2*R*-2-(*N*-Isopropylamino)-1-phenylpropanol 5. $PtCl_2$ (0.375 g, 1.4 mmol, 3.6 mol %) was fully hydrogenated in EtOH 15 mL, for approximately 15 min) to afford a black suspension. The solvent was removed *via* cannula, and the black solid was washed with two portions of EtOH (7.5 mL) to remove HCl. 1*R*,2*R*-2-Amino-1-phenylpropanol **4** (6 g, 39.7 mmol, ex B·HCl, Sigma) was dissolved in EtOH (15 mL) and Me_2CO (3.4 mL). The resulting solution was added to the colloidal platinum in EtOH (6 mL) in a Schlenk tube under argon. The degassed reaction mixture was stirred under H_2, and after 18 h at ambient temperature 1150 mL (1.3 mol equiv) had been adsorbed. The reaction was degassed and then filtered through a large plug of Celite which was washed with EtOH (30 mL). The filtrate was combined with the washings and evaporated to afford a viscous oil which was distilled, collecting the title compound at 98 °C, 0.004 mmHg as a very hygroscopic white crystalline solid (7.3 g, 96%): $[\alpha]^{20}_D$ −152.12 (*c* 1.06, $CHCl_3$); ^{1}H NMR (200 MHz, $CDCl_3$) 7.35 (5H, m, C_6H_5), 4.41 (1H, d, *J* 8.6 Hz, C_6H_5CH), 2.94 (1H, q of q, *J* 6.5, 7.9 Hz, $(CH_3)_2CHN$), 2.68 (1H, dq, *J* 8.6, 6.3 Hz, C_6H_5CHCH), 1.12 (3H, d, *J* 6.5 Hz, $(CH_3)_2CHN$), 1.05 (3H, d, *J* 7.9 Hz, $(CH_3)_2CHN$) and 0.96 (3H, d, *J* 6.3 Hz, $C_6H_5CHCHCH_3$). Anal. Calcd for $C_{12}H_{19}NO$ C, 74.57; H, 9.91; N, 7.25. Found: C, 74.28; H, 9.90; N, 7.69.

4*R*,5*R*-4-Methyl-3-isopropyl-5-phenyloxazaborolidine 6. 1*R*,2*R*-2-(*N*-Isopropylamino)-1-phenylpropanol (**5**) (10.5 g, 54.4 mmol) was placed in a Schlenk tube. After evacuating and purging with argon (three cycles), THF (10 mL) was added *via* syringe to afford a partial solution. The sample was cooled to 0 °C and then $BH_3{\cdot}SMe_2$ (Aldrich, 2.0 M in THF, 27.2 mL, 54.36 mmol) added by cannula over a period of 3 h. The reaction mixture was stirred at room temperature for 36 h after which 1 equiv of H_2 gas had evolved. Volatile material was removed *in vacuo* to give a white foam. The vessel was purged with argon and then heated to 120 °C for 2.5 h after which a further 1 equiv of H_2 gas had been produced, affording a clear colorless oil. This was transferred *via* cannula to a vacuum jacketed Vigreux column, and the product was distilled as a clear colorless mobile oil bp 65 °C, 0.015 mmHg (8.98 g, 81%, $\rho \approx 0.97$ g cm^{-3}): $[\alpha]^{20}_D$ −59.7 (*c* 0.98, $CHCl_3$); ^{1}H NMR (500 MHz, $CDCl_3$) 7.38 (5H, m, C_6H_5), 4.91 (1H, d, *J* 6.73 Hz, C_6H_5CH), 3.49 (1H, q of q, *J* 6.41 Hz, $(CH_3)_2CHN$), 3.25 (1H, dq, *J* 6.73, 6.35 Hz, C_6H_5CHCH), 1.34 (3H, d, *J* 6.41 Hz, CH_3CHN), 1.29 (3H, d, *J* 6.41 Hz, CH_3CHN) and 1.12 (3H, d, *J* 6.35 Hz, $C_6H_5CHCHCH_3$); ^{13}C NMR (125 MHz, $CDCl_3$) 143.6 (C ipso), 128.4 (C ortho), 127.6 (C para), 125.5 (C meta), 87.6 (C_6H_5CH), 61.4 (C_6H_5CHCH), 43.8 ($(CH_3)_2CHN$), 24.2 ($(CH_3)_2$-CHN), 23.4 ($C_6H_5CHCHCH_3$) and 19.9 ($(CH_3)_2CHN$); ^{11}B NMR (80.21 MHz, C_6D_6) 28.4 (d, J_{B-H} 151 Hz); IR (thin film) 2580 cm^{-1} (B-H); GCMS (BP1 12m, 70–240 °C, 20° min^{-1}, EI$^+$, room temperature 459s) 204 (3), 203.09 (15, M$^+$), 202 (6, M$^+$), 189 (10), 188 (100, M − CH_3), 187 (32, M − CH_3).

(2-[$^2H_1$])-4-Methoxyphenylethyne. 4-Methoxyphenylethyne (2.0 g, 15.2 mmol)[44] was dissolved in CH_3OD (Aldrich >99.8 atom %, 20 mL) under argon. LiH (Fluka, *ca.* 8 mg (*ca.* 1 mmol) was added resulting in vigorous production of HD. The colorless solution was left at ambient temperature for 12 h, and then the volatiles were stripped *in vacuo* to yield a white solid and oil. The reaction vessel was then twice recharged with CH_3OD and stripped to vacuum after a 12-h period. D_2O (Fluorochem >99.9 atom %, 2 mL) was added, and the mixture was extracted with hexane (3 × 10 mL). The combined organics were washed with D_2O (2 × 2 mL) and then dried ($MgSO_4$). Removal of the solvent *in vacuo* afforded a clear colorless oil (1.92 g, 95%); ^{1}H NMR (500 MHz, $CDCl_3$) 7.46 (2H, d, *J* 8.8 Hz, C*H* ortho), 6.86 (2H, d, C*H* meta) and 3.83 (3H, s, CH_3O); ^{2}H NMR (76 MHz, $CDCl_3$) 3.0 (s, C*CD*); ^{13}C NMR (125 MHz, $CDCl_3$) 160.0 (C ipso), 133.6 (HC ortho), 114.3 (C para), 114.0 (HC meta) 83.3 (t, J_{CCD} 7.3 Hz , *C*CD,), 75.4 (t, J_{CD} 39 Hz, C*C*D) and 55.3 (H_3CO); GC-MS (BP1 40–41 °C (0.5 °C min^{-1}), 41–180 °C (10 °C min^{-1}, room temperature 356 s) EI$^+$, 134 (8.5), 133 (100).

((*E*)-1,2-[$^2H_2$])-4-Methoxyphenylethene. 4-Methoxyphenylethyne (2 g, 15.15 mmol) and cyclooctadienebis(methyldiphenylphosphine)rhodium tetrafluoroborate (80 mg, 0.114 mmol) in 2-methoxyethanol (15 mL) were degassed together and allowed to equilibrate thermally under D_2 in a Schlenk tube. Vigorous stirring was commenced, and D_2 uptake was monitored. The reaction was terminated when a sharp change in rate was observed. Water (20 mL) was added, and the mixture was extracted with isopentane (4 × 20 mL). The combined organics were dried ($MgSO_4$) and solvent removed *in vacuo* to afford an orange oil. Distillation in vacuo into a liquid N_2 trap gave a clear colorless liquid (1.2 mL, 1.218 g, 59%): ^{1}H NMR (300 MHz, $CDCl_3$) 7.36 (2H, d, *J* 8.73 Hz, C*H* ortho), 6.87 (2H, d, CH meta), 5.59 (1H, t, *J* 2.595 Hz, C=C*H*-E) and 3.82 (3H, s, CH_3O); ^{2}H NMR (76 MHz, $CDCl_3$) 6.8 (d, J_{D-H} 2.4 Hz, ArC*D*) and 5.2 (s, C=C*D*); ^{13}C NMR (50 MHz, $CDCl_3$) 159.7 (C *ipso*), 136.1 (t, J_{CD} 24 Hz, *C*DCDH), 130.6 (C *para*), 127.6, HC *ortho*), 114.1 (HC *meta*), 111.3 (t, J_{CD} 25 Hz, CD*C*DH) and 55.3 (H_3C); IR (thin film) 1611 (CD=CDH) ({CH=CH_2} = 1608) cm^{-1}; GC-MS (BP1 80–200 °C (5 °C min^{-1}, room temperature 166 s) EI$^+$, 137 (11.22), 136 (100).

(1,2,2-[$^2H_3$])-4-Methoxyphenylethene was prepared in a similar fashion to the above example. 2-[$^2H_1$]-4-methoxyphenylethyne (400 mg, 3 mmol) and cyclooctadienebis(methyldiphenylphosphine)rhodium tetrafluoroborate (16 mg, 22.9 μmol) in d_6-acetone (Aldrich >99.8 atom %, 3.38 mL) (0.344 mL, 352 mg, 82%); ^{1}H NMR (500 MHz, $CDCl_3$) 7.39 (2H, d, *J* 6.67 Hz, C*H* ortho), 6.90 (2H, d, C*H* meta,) and 3.84 (3H, s, CH_3O); ^{2}H NMR (76 MHz, $CDCl_3$) 6.7 (s, ArC*D*), 5.7 (s, ArCDCD*-Z*), and 5.2 (s, ArCDCD*-E*); ^{13}C NMR (125 MHz, $CDCl_3$) 159.5 (C *ipso*), 135.8 (t, J_{CD} 25 Hz, *C*DCD$_2$), 130.4 (C *para*), 127.4 (HC *ortho*), 113.9 (HC *meta*), 111.3 (CDCD$_2$, m) and 55.2 (H_3C); IR (thin film) 1611 (DC=CD_2) ({CH=CH_2} = 1608) cm^{-1}; GC-MS (BP1 40–41 °C (0.5 °C min^{-1}) then 41–180 °C (10 °C min^{-1}, room temperature 363 s) EI$^+$, *m*/*z* 138 (8.2) 137 (100).

((*E*)-2-[$^2H_1$])-4-Methoxyphenylethene was prepared in a similar fashion to the above using H_2 (441 mg, 87%): ^{1}H NMR (500 MHz, $CDCl_3$) 7.35 (2H, d, *J* 8.69, C*H* ortho), 6.87 (2H, d, C*H* meta), 6.66 (1H, dt, *J* 10.9, 2.57 Hz, ArC*H*), 5.11 (1H, d, *J* 10.9 Hz, ArC=C*H*), and 3.81 (3H, s, CH_3O); ^{2}H NMR (76 MHz, $CDCl_3$) 5.7 (d, J_{D-H} 2.6 Hz, C=C*D*); ^{13}C NMR (125 MHz, $CDCl_3$) 158.8 (*C ipso*), 136.2 (*C*HCDH), 130.3 (HC *para*), 127.4 (HC *ortho*), 113.9 (HC *meta*), 111.2 (t, J_{CD} 24 Hz, CD*C*DH), and 55.2 (H_3C); IR (thin film) 1608 (HC=CDH), ({CH=CH_2} = 1608) cm^{-1}; GC-MS (BP1 40–41 °C (0.5 °C min^{-1}), 41–180 °C (10 °C min^{-1}, room temperature 363 s) EI$^+$136 (8.36), 135 (100.0).

(*E*)-(4*R*,5*R*-3-Isopropyl-4-methyl-5-phenyl-1,3,2-oxazaborolidyl)(4-methoxyphenyl) ethene 9. Tetrakis(η^2-ethene)di-μ-chlorodirhodium (2.3 mg, 5.9 μmol) was placed in a 5-mL vial, and the vial was evacuated and then flushed with argon (three cycles). C_7H_8 (2.5 mL) was added followed by 4-methoxyphenylethene **1** (475 μL, 3.54 mmol) to afford a bright orange solution of rhodium complex **7** (0.48 mol %). Oxazaborolidine **6** (260 μL, 250 mg, 1.23 mmol) was added *via* microsyringe resulting in a red-brown solution that darkened over 5 min to a deep rust-brown color. After 4 h, the reaction was transferred *via* cannula into a distillation bulb under argon in a Kugelröhr oven. The pressure was reduced to remove residual hydrocarbons (75 °C, 0.04 mBar). The title compound was collected at 250 °C (oven T), 0.035 mBar as a viscous clear oil (404 mg, 98%): $[\alpha]^{23}_D$ −106.5 (*c* 0.7, $CHCl_3$): ^{1}H NMR (300 MHz, C_6D_6) 7.89 (1H, d, *J* 18.1 Hz, ArC*H*CHB), 7.42 (2H, d, 8.65 Hz, ring A *ortho* C*H*), 7.32 (1H, t, *J* 7.3 Hz, ring B *para* C*H*), 7.18 (4H, m, ring B *ortho* and *meta* C*H*), 6.73 (2H, d, *J* 8.69 Hz, ring A *meta* C*H*), 6.55 (1H, d, *J* 18.09 Hz, ArCHC*H*B), 4.89 (1H, d, *J* 5.6 Hz, ArC*H*OB), 3.36 (2H, m,

ArCHC*H*NB and NC*H*$(CH_3)_2$), 3.26 (3H, s, CH_3OC) and 1.10 (9H, m, ArCHCHCH_3 and NCH$(CH_3)_2$); ^{13}C NMR (125 MHz, C_6D_6) 160.6 (CH_3OC), 146.9 (Ar*C*HCHB), 144.1 (ring B *ipso*), 131.7 (ring A *ipso*), 128.6 (ring B *ortho C*H), 128 (ring B *meta* and *para C*H), 127.1 (ring A *ortho C*H), 116 (br, ArCH*C*HB), 86.1 (ArCH*O*B), 63.3 (ArCH*C*H-NB), 54.8 (CH_3OC), 45.2 (N*C*H$(CH_3)_2$), 24.9 (ArCHCH*C*H_3), 23.3 (NCH$(CH_3)_2$) and 22.4 (NCH$(CH_3)_2$); ^{11}B NMR (80.21 MHz, C_6D_6) 30.6 (bs); IR (thin film on NaCl) 1621 cm^{-1} (C=CB) 1605 (C=C Ar) cm^{-1}; GCMS BP1 12m 140–260 °C (20 °C min^{-1} room temperature 365 s) EI$^+$ m/z 335 (M^+). Anal. Calcd for $C_{21}H_{26}BNO_2$: C, 75.27; H, 7.77; N, 4.18. Found: C, 74.92; H, 8.1; N, 4.15.

(*E*)-(4*R*,5*R*-3-Isopropyl-4-methyl-5-phenyl-1,3,2-oxazaborolidyl)(4-chlorophenyl)ethene 11 was prepared similarly: bp 200 °C (oven), 0.025 mmHg as a viscous clear colorless oil (459 mg, 100%); $[\alpha]^{24}_D$ −111.58 (*c* 1.165, $CHCl_3$); ^{1}H NMR (300 MHz, C_6D_6) 7.65 (1H, d, *J* 18.1 Hz, ArC*H*CHB), 7.36 (2H, d, *J* 7.47 Hz, ring A *meta C*H), 7.21 (1H, t, *J* 7.11 Hz, ring B *para C*H), 7.12 (4H, m, ring B *ortho* and *meta C*H), 7.10 (2H, d, *J* 8.64 Hz, ring A *ortho C*H), 6.49 (1H, d, *J* 18.11 Hz, ArCHC*H*B), 4.86 (1H, d, *J* 5.71 Hz, ArC*H*OB), 3.36 (1H, dq, *J* 6.00, 5.71 Hz, ArCHC*H*NB), 3.29 (1H, m, NC*H*$(CH_3)_2$) and 1.07 (9H, m, ArCHCHCH_3 and NCH$(CH_3)_2$); ^{13}C NMR (125 MHz, C_6D_6) 145.6 (Ar*C*HCHB), 144.3 (ring B *ipso*), 137.2 (Cl*C*), 134.3 (ring A *ipso*), 128.7 (ring A *ortho C*H), 128.3 (ring B *ortho C*H), 120 (br, ArCH*C*HB), 128 (ring B *meta* and *para C*H), 86.1 (ArCH*O*B), 63.3 (ArCH*C*HNB), 45.1 (N*C*H$(CH_3)_2$), 25.0 (ArCHCH*C*H9) and 22.3 (NCH$(CH_3)_2$); ^{11}B NMR (80.21 MHz, C_6D_6) 31 (bs); IR (thin film) 1620 (C=CB, C=C Ar); GCMS BP1 12m 140–260 °C (20° min^{-1} room temperature 410 s) EI$^+$ m/z 339 (M^+). Anal. Calcd for $C_{20}H_{23}BNClO$: C, 70.72; H, 6.83; N, 4.12. Found C, 70.48; H, 6.78; N, 4.41%.

(*E*)-(4*R*, 5*R*-3-Isopropyl-4-methyl-5-phenyl-1,3,2-oxazaborolidyl)(ferrocenyl)ethene 13 was prepared similarly: bp 250 °C (oven), 0.020 mmHg as a highly viscous deep red oil (59 mg, 38%); ^{1}H NMR (300 MHz, C_6D_6) 7.71 (d, 1H, *J* 17.8 Hz, CpC*H*CHB), 7.43 (5H, m, C_6H_5), 6.31 (1H, d, CpCHC*H*B), 4.90 (1H, d, *J* 5.0 Hz, C_6H_5C*H*OB), 4.44 (2H, brm, Cp-2-H), 4.34 (2H, brm, Cp-3-H), 3.99 (5H, s, Cp′), 3.36 (2H, C_6H_5CHC*H*NB and $(CH_3)_2$C*H*N) and 1.10 (9H, s, s, C_6H_5-CHCHCH_3 and $(CH_3)_2$CHN); MS (200 °C heated probe) EI$^+$ m/z 413 (M^+) (MS fits predicted isotope cluster for $C_{24}H_{28}OBFe$) m/z found 413.1615, $C_{24}H_{28}OBFe$ requires 413.1613.

(*E*)-(*p*-Methoxyphenyl)etheneboronic Acid 10. (*E*)-(4*R*,5*R*-3-Isopropyl-4-methyl-5-phenyl-1,3,2-oxazaborolidyl)(4-methoxyphenyl)ethene (**9**) (172 mg, 0.484 mmol) was mixed with water (2.5 mL) and NaOH (3 mol dm^{-3}, 0.15 mL). After heating to 100 °C (10 min) the mixture was cooled and acidified to pH 2–3 with aqueous HCl resulting in precipitation of a white solid which was collected by filtration, recrystallized from boiling water, and dried *in vacuo* to afford the title compound as a white crystalline solid (81 mg, 94%, mp 187–188.5 °C. ^{1}H NMR (500 MHz, C_3D_6O) 7.45 (2H, d, *J* 8.62 Hz, C*H ortho*), 7.32 (1H, d, *J* 18.27 Hz, C_6H_4C*H*CHB), 6.92 (2H, d, *J* 8.65 Hz, C*H meta*), 6.88 (2H, s, C_6H_4-CHCHB(O*H*)$_2$), 6.05 (1H, d, *J* 18.33 Hz, C_6H_4CHC*H*B), and 3.81 (3H, s, CH_3OC); ^{13}C NMR (125 MHz, C_3D_6O) 160.8 (CH_3OC), 146.9 (C_6H_5CHCHB), 131.6 (*C* ipso), 128.6 (*CH ortho*), 119.8 (bs, C_6H_5-CHCHB), 114.6 (*CH meta*), and 55.3 (CH_3OC); ^{11}B NMR (80.21 MHz, C_3D_6O) 28.3 (bs); IR (KBr disc) 1622 (C=CB) and 1603 cm^{-1} (C=CAr); MS (200 °C heated probe) EI$^+$ m/z 178 (M^+) (MS fits predicted isotope cluster for $C_9H_{11}BO_3$). Anal. Calcd for $C_9H_{11}BO_3$: C, 60.75; H, 6.19. Found: C, 60.98; H, 5.96.

(*E*)-(4-Chlorophenyl)etheneboronic acid 12 was prepared similarly as a white crystalline solid (108 mg, 96%): mp 210–212 °C; ^{1}H NMR (500 MHz, C_3D_6O) 7.53 (1H, d, *J* 8.47 Hz C*H meta*), 7.39 (2H, d, *J* 8.48 Hz, C*H ortho*), 7.35 (1H, d, *J* 18.43 Hz, C_6H_4C*H*CHB), 7.04 (2H, s, C_6H_4CHCHB(O*H*)$_2$), and 6.23 (1H, d, *J* 18.32 Hz, C_6H_4CHC*H*B); ^{13}C NMR (125 MHz, C_3D_6O) 145.6 (C_6H_4*C*HCHB), 137.6 (Cl*C*), 134.1 (*C ipso*), 129.2 (*CH* meta), 128.8 (*CH ortho*), and 123.9 (bs, C_6H_4-CH*C*HB); ^{11}B NMR (80.21 MHz, C_3D_6O) 27.9 (bs); IR (KBr disc) 1621 cm^{-1} (C=CB, C=C Ar). MS (200 °C heated probe) EI$^+$ m/z 182 (M^+) (MS fits predicted isotope cluster for $C_8H_8O_2BCl$. Anal. Calcd for $C_8H_8O_2BCl$: C, 52.67; H, 4.42. Found: C, 52.88; H, 4.15.

Ferrocenylethaneboronic acid 14 was prepared similarly as bright orange plates (19.7 mg, 80%): mp 154–156 °C; ^{1}H NMR (500 MHz, C_3D_6O) 7.17 (1H, d, *J* 18.2 Hz, CpC*H*CHB), 6.75 (2H, s, CpCHCHB(O*H*)$_2$), 5.74 (1H, d, CpCHC*H*B), 4.44 (2H, A of AA′BB′, *J* ca. 1.8 Hz, Cp-2*H*), 4.27 (2H, B of AA′BB′, Cp-3*H*), and 4.09 (5H, s, Cp′ C*H*); ^{13}C NMR-(125 MHz, C_3D_6O) 146.5 (Cp*C*HCHB), 119.3 (bs, CpCH*C*HB), 84.3 (Cp *ipso C*), 69.7 (Cp 2-*C*H and 3-*C*H), and 67.8 (Cp′ *C*H); ^{11}B NMR (80.21 MHz, C_3D_6O) 27.9 (bs); IR (KBr disc) 1622 cm^{-1} (C=CB); MS (200 °C heated probe) EI$^+$ m/z 256 (M^+); MS fits predicted isotope cluster for $C_{12}H_{23}O_2BFe$. Anal. Calcd for $C_{12}H_{23}O_2BFe$: C, 56.32; H, 5.12. Found: C, 56.23; H, 5.03.

Typical Procedure for the Reaction of Labeled Alkene with Oxazaborolidine 6. A suspension of tetrakis(η^2-ethene)di-μ-chlorodirhodium (7.5 μmol) in d_8-toluene, 200 μL in a 1000-μL graduated flask attached to the vacuum line, under argon was treated with (1,2,2-[^{2}H]$_3$)-**1** (21 mg, 20 μL, 0.153 mmol) to afford a deep red solution of dimeric tetrakis-(η^2-(1,2,2-[^{2}H]$_3$)-(*p*-methoxyphenyl)ethene)di-μ-chlorodirhodium (**7**). The cherry-red solution was accurately diluted to a total volume of 1000 μL with d_8-toluene, transferred into a 1.5-mL vial under argon, and then sealed with a septum cap. (1,2,2-[^{2}H]$_3$)-(4-Methoxyphenyl)ethene (50 mg, 51 μL, 0.373 mmol) was injected into a 5-mm NMR tube attached to the vacuum line under argon. d_8-Toluene (400 μL) was added *via* microsyringe, resulting in a colorless solution, unchanged by addition of oxazaborolidine **6** (48 mg, 50 μL, 0.236 mmol). The NMR tube was sealed with a tapered bung, under argon, and a ^{1}H NMR (500 MHz) spectrum was acquired. Fifty microliters of the catalyst solution was added, resulting in a pale straw-yellow solution. The reaction was monitored by ^{1}H NMR (500 MHz) and then left at ambient temperature for 12 h. The resulting pale brown solution was transferred into a distillation bulb attached *via* a "U-tube" trap to the vacuum line, under argon, treated with β-naphthol (*ca.* 50 mg), then stirred at ambient temperature for 20 min. The U-tube trap was immersed in a bath of liquid nitrogen, and the system was evacuated for 10 min. Its contents (a solution of deuterated alkane in C_7D_8) were then analyzed by ^{1}H NMR.

Kinetic Experiments (Figure 9). The following procedure is typical: A stock solution of tetrakis(η^2-**1**)-di-μ-chlorodirhodium (**7**) (0.0373 M) was prepared in C_7D_8. A 500-μL NMR sample in C_7D_8 was made up from stock solutions of 4-methoxyphenylethene **1** and oxazaborolidine **6** to provide initial concentrations (subsequent to catalyst addition) of 0.46 M in the latter and 0.75 M in the former. The tube was then sealed under argon, with a 10-mm tapered solid neoprene bung. The exposed section of the bung (*ca.* 3 mm) was then removed with a scalpel. After the tube had thermally equilibrated to 25 °C in the probe of the NMR spectrometer, ^{1}H NMR spectrum was acquired (32 pulses). The tube was then removed, and an automated time series acquisition program was loaded and held on "standby". A 10-μL aliquot of the catalyst solution was loaded, under argon, into the barrel of a microsyringe with a 140-mm fine needle. The needle was inserted through the bung of the NMR tube until the needle tip was *ca.* 5 mm from the surface of the solution and rapidly injected, and the resulting straw-yellow solution thoroughly mixed and reinserted into the spectrometer. The spectrometer was reshimmed, the whole process (including catalyst addition) taking ca. 85 s. The automated software was immediately initiated, and a total of 15 sets of 32 FID pulses performed at 133-s intervals for a total of 2000 s.

The concentration of oxazaborolidine **6** was estimated by integrating the oxazaborolidine ring benzylic resonance of reactant **6** (4.75 ppm) against that of product **9** (4.80 ppm) in the ^{1}H NMR spectrum.

2-[^{2}H$_1$]-Benzodioxaborole. Freshly sublimed 1,2-dihydroxybenzene (3.6 g, 32.7 mmol) was dissolved in THF (11.0 mL) in a Schlenk tube under argon and transferred dropwise *via* cannula into a second Schlenk tube containing BD_3·THF in tetrahydrofuran (1.07 mol dm^{-3},40 mL) under argon at 0 °C over a period of 5 h. After complete addition the reaction mixture was warmed to ambient temperature and stirred until HD evolution had ceased (24 h). Tetrahydrofuran was removed by distillation under a slightly positive argon pressure until a 10-mL residue was obtained. This was transferred *via* cannula into a one piece micro-Vigreux distillation set and distillation continued until no more tetrahydrofuran condensed (66–67 °C). The pressure was then reduced to 175 mmHg and the product was collected at 80 °C to afford a clear colorless liquid (2.4 g, 61%): mp 14 °C; ^{1}H NMR (500 MHz, C_6D_6) 6.98 (2H, dd, *J* 5.32, 3.31 Hz, C*H* ortho) and 6.74 (2H, dd, C*H* meta); ^{2}H NMR (76 MHz, C_6D_6) 4.6 (bs); ^{11}B NMR (80.21 MHz, C_6D_6) 28.6 (s). IR(thin film) 1884 (B-D) cm^{-1}; GC-MS BP11 12m 35–36 °C (0.5 °C min^{-1}), 36–180 °C (20 °C min^{-1}, room temperature 135 s) EI$^+$ 122 (6.06), 121 (100), 120 (40.37). Found: C, 59.6; H, 4.5. $C_6H_4D_1BO_2$ requires C, 59.8; H, 4.9.

3,4,5,6-[^{2}H$_4$]-1,2-Dihydroxybenzene. This was prepared by a modification of the literature method:[25] ^{1}H NMR (300 MHz, $CDCl_3$) 5.35 (2H, CO*H*, s); ^{13}C NMR (125 MHz, CD_3OD) 146.2 (*C* ipso), 120.5 (t, J_{CD} 24.4 Hz, D*C* meta), and 116.1 (t, J_{CD} 23.9 Hz, DC ortho); ^{2}H NMR (76 MHz, CD_3OD/CH_3OH) 6.8 (br s) and 6.7 (br s); GC-MS, (BP1 80–120 °C (0.5 °C min^{-1}, room temperature 270 s) EI$^+$ 115 (8.2), 114 (100.00), and 113 (7.87).

2,3′,4′,5′,6′-[^{2}H$_5$]Benzodioxaborole. From the above and BD_3·THF

as described earlier: 3,4,5,6-[$^2H_4$]-1,2-Dihydroxybenzene (2.05 g, 17.95 mmol) was dissolved in THF (5.6 mL) in a Schlenk tube under argon and transferred dropwise *via* filtering cannula into a second Schlenk tube containing BD_3·THF in THF (1.26 mol dm^{-3}, 14.5 mL) under argon at 0 °C over a period of 120 min. Workup and distillation as before gave the product (230 mg, 10.2%); ^{13}C NMR (125 MHz, d_8-toluene) 147.9 (*ipso*), 122.7 (t, J_{CD} 24.6 Hz, *meta*), and 112.5 (t, J_{CD} 25.0 Hz, D*C ortho*); ^{11}B NMR (80.21 MHz, d_8-toluene) 28.6 (s); GC-MS BP1 12m 35–36 °C (0.5 °C min^{-1}) 36–180 °C (20 °C min^{-1}, room temperature 120 s) EI^+ 126 (6.34), 125 (100.00), 124 (39.51), and 123 (3.54).

Catalyzed Addition of Catecholborane to Alkene 1. The following procedure is typical: To a freshly distilled sample of alkene **1** (0.050 g; 0.373 mmol) and freshly distilled **HBcat** (25 μL, 26.8 mg, 0.224 mmol) in C_7D_8 (0.40 mL) was added 50 μL of a stock solution of catalyst **7** (11.6 mg mL^{-1}, 0.09 mol%) to give an yellow solution which changed to a brown coloration within 3 min at ambient temperature. The mixture was analyzed by ^1H NMR at 500 MHz within 2 h, estimating the relative proportions of the product components by integration of the four separate OMe groups at 3.28 (**23**), 3.31 (**1**), 3.33 (**24**), and 3.36 (**8**) ppm. The ratios were confirmed by integration of separate resolved signals for the individual components. Samples handled in this way showed equivalent yields of alkane **8** and vinylborane **23**; on standing for 12 h, the proportion of vinylborane decreased and that of primary borane **24** was enhanced.

(Benzo-1,3,2-dioxoborolidyl)-(*E*)-2-(4-methoxyphenyl)ethene 23. Compared with an authentic sample prepared from the alkyne and **HBcat** (90 °C, 1 h; Dr. T. Layzell unpublished work) which was correlated with the boronic acid **10** (H_2O, 25 °C, 1 h). From these experiments: ^1H NMR (500 MHz, C_7D_8) 7.72 (1H, d, *J* 18.4 Hz, C*H*CHB,), 7.71 (2H, A of AA′BB′, ring B), 6.94 (2H, d, *J* 8.8 Hz, ring A C*H* meta), 6.84 (2H, B of AA′BB′, ring B), 6.64 (2H, d, ring A C*H ortho*), 6.29 (1H, d, CHC*H*B), and 3.28 (3H, s, CH_3O); ^{13}C NMR (C_7D_8) 161.4 (C-O *ipso*), 152.1 (*C*=CB), 149.1 (C-OB *ipso*), 130.4 (C-C *ipso*), 129.3 (3-ArOMe), 122.8 (3,4 *cat*), 114.4 (2,5 *cat*), 112.6 (2-ArOMe); ^{11}B NMR (80.21 MHz, C_7D_8) 35 (br s); GC-MS BP1 12m 35–36 °C (0.5 °C min^{-1}) 36–180 °C (20 °C min^{-1}, room temperature 944 s) EI^+ 252; M^+ MS (probe EI^+, *T* = 30 °C) 252 (M^+).

(Benzo-1,3,2-dioxoborolidyl)-2-(4-methoxyphenyl)ethane 24:[12] ^1H NMR (500 MHz, C_7D_8) 7.00 (2H, d, *J* 8.7 Hz, ring A C*H* meta), 7.00 (2H, dd, A of AA′BB′, ring B), 6.80 (2H, B of AA′BB′), 6.70 (2H, d, ring A C*H* ortho), 3.33 (3H, s, CH_3O), 2.76 (2H, t, *J* 8.24 Hz, CH_2-CH_2B), and 1.40 (3H, t, CH_2CH_2B); ^{11}B NMR (80.21 MHz, C_7D_8) 35 (br s); GC-MS BP1 12m 35–36 °C (0.5 °C min^{-1}) 36–180 °C (20 °C min^{-1}, room temperature 773 s) EI^+ 254; M^+ MS (probe EI^+, *T* = 30 °C) 254 (M^+).

1-[$^2H_1$]Triethylsilane. $LiAlD_4$ (Koch-Light, >99.5 atom % D, 900 mg, 21.45 mmol) was placed in a Schlenk tube. After evacuating and flushing with argon (three cycles), diethyl ether (5 mL) was added *via* syringe, and the resulting suspension was vigorously stirred. $Et_3SiOSO_2CF_3$ (1.7 mL, 1.98 g, 7.5 mmol) was added *via* syringe to the above suspension at 25 °C over a period of 300 s resulting in a slightly exothermic reaction and foaming. After complete addition the thick suspension was stirred at ambient temperature for 12 h. The reaction mixture was then filtered *via* an on-line sinter plate under argon into a second Schlenk tube. The grey solid remaining on the plate was washed with Et_2O (2 × 2.5 mL). [CAUTION: FILTRATE IS EXTREMELY REACTIVE]. The combined filtrate and washings were transferred *via* cannula into a one piece vacuum jacketed Vigreux kit under argon. The diethyl ether was removed by distillation under a slight positive pressure of argon to afford a white solid residue. The title product was then collected at 105 °C as a clear colorless mobile oil (550 mg, 63%), keeping the bath temperature as low as feasible. The isotopic purity of Et_3SiD was estimated to be 99.6 atom % D by integration of ^{29}Si satellites in ^1H NMR (500 MHz, C_6D_6) of $PhMe_2SiH$ against residual Et_3SiH signal in a 50:50 mixture of $PhMe_2SiH$ and Et_3SiD: ^1H NMR (300 MHz, C_6D_6) 0.98 (9H, t, *J* 7.9 Hz) and 0.54 (6H, q, *J* 7.9 Hz); ^2H NMR (76 MHz, $CDCl_3$) 3.7 (1[^2H], s); ^{13}C NMR (125 MHz ($CDCl_3$) 8.1 (CH_3CH_2) and 2.4 (CH_3CH_2); MS EI^+ (heated probe) *m/z* (119 (0.08), 118 (0.83), 117 (8.26), 116 (1.51), and 115 (5.57); IR (thin film) 1531 cm^{-1} (Si–D), {no band observable at 2103 cm^{-1} (Si–H)}.

Preparative Scale Hydrosilylation 4-Methoxyphenylethene **1** (800 mg, 5.97 mmol) was injected into a 10-mL ampoule, connected to the vacuum line, under argon. Benzene (7 mL) was added followed by Et_3SiH (1.75 mL, 1.27 g, 10.96 mmol) to afford a clear colorless solution. Tetrakis-(η^2-ethene)di-μ-chlorodirhodium (16 mg, 41 μmol) was placed in a 2.5-mL vessel under argon, and benzene (1 mL) was added. Upon treatment with (*p*-methoxyphenyl)ethene **1** (200 μL, 200 mg, 1.5 mmol) a clear red solution of dimeric tetrakis(η^2-(*p*-methoxyphenyl)ethene)di-μ-chlorodirhodium **7** was produced, with gas evolution. The solution was filtered *via* cannula into the above ampoule resulting in a bright yellow solution. After 18 h at ambient temperature the reaction had deposited a small amount of brown solid with a golden yellow-orange supernatant. The solution was transferred *via* cannula into a vacuum jacketed Vigreux, and solvent was removed *in vacuo*. The pressure was then further reduced, and four fractions were collected at 90–91 °C, 0.025 mmHg. Analytically pure samples of each component were obtained by preparative GC separation: OV1 7 ft 142 °C (post column outlet at 200 °C) with N_2 carrier at constant 1.3 atm and maximum injection volumes of 20 μL of a 50/50 v/v solution of fraction 3 in Et_2O.

(*E*)-2-(*p*-Methoxyphenyl)triethylsilylethene 28: clear colorless oil; ^1H NMR(300 MHz, $CDCl_3$) 7.39 (2H, d, *J* 8.69 Hz, *ortho* C*H*), 6.87 (2H, d, *J* 8.72 Hz, *meta* C*H*), 3.83 (3H, s, CH_3O), 6.84 (1H, d, *J* 19.28 Hz, $CH_3OC_6H_4CHCHSi$), 6.26 (1H, d, *J* 19.31 Hz, $CH_3OC_6H_4$-CHC*H*Si), 0.99 (9H, t, *J* 7.66 Hz, CH_3CH_2Si), and 0.66 (6H, q, *J* 7.96 Hz, CH_3CH_2Si); ^{13}C NMR (125 MHz, $CDCl_3$) 159.6 (CH_3OC), 144.3 ($CH_3OC_6H_4CHCHSi$), 131.8 (*C ipso*), 127.5 (*C ortho*), 123.2 (CH_3-$OC_6H_4CHCHSi$), 114.0 (*C* meta), 55.3 (CH_3O), 7.4 (CH_3CH_2Si), and 3.7 (CH_3CH_2Si); ^{29}Si NMR (49.69 MHz, C_6D_6) –0.15 (s); IR (thin film) 1607.0 cm^{-1} (C=C) and (C=CAr); GCMS (BP1 12m 140 °C room temperature 650 s, EI^+) *m/z* 248 (M^+). Anal. Calcd for $C_{15}H_{24}$-OSi C, 72.52; H, 9.74 Found C, 72.85; H, 9.89%.

2-(*p*-Methoxyphenyl)triethylsilylethane 29: clear colorless oil; ^1H NMR (300 MHz, $CDCl_3$) 7.13 (2H, d, *J* 8.49 Hz, ortho C*H*), 6.83 (2H, d, *J* 8.60 Hz, meta C*H*), 3.80 (3H, s, CH_3O), 2.57 (2H, t, *J* ca. 8.5 Hz, $CH_3OC_6H_4CH_2$), 0.96 (9H, t, CH_3CH_2Si), 0.87 (2H, t, $CH_3OC_6H_4$-CH_2CH_2), and 0.56 (6H, q, *J* 7.7 Hz, CH_3CH_2Si); ^1H NMR (125 MHz, $CDCl_3$) 157.7 (CH_3OC), 137.8 (*C ipso*), 128.6 (*C ortho*), 113.8 (*C meta*), 55.3 (CH_3O), 29.1 ($CH_3OC_6H_4CH_2$), 13.9 ($CH_3OC_6H_4CH_2CH_2$), 7.4 (CH_3CH_2Si), and 3.4 (CH_3CH_2Si); ^{29}Si NMR (49.69 MHz, C_6D_6) 6.83 (s); IR (thin film) 1611 cm^{-1} (C=C Ar); GCMS (BP1 12m 140 °C room temperature 384 s, EI^+) *m/z* 250 (M^+). Anal. Calcd for $C_{15}H_{26}OSi$ C, 71.93; H, 10.46 Found C, 71.62; H, 10.79%.

1-(*p*-Methoxyphenyl)triethylsilylethane 30: clear colorless oil; ^1H NMR (300 MHz, $CDCl_3$) 6.70 (2H, d, *J* 8.6 Hz, *ortho* C*H*), 6.81 (2H, d, *J* 8.70 Hz, *meta* C*H*), 3.79 (3H, s, CH_3O), 2.25, (1H, q, *J* 7.62 Hz, CH_3-OC_6H_4CHSi), 1.35 (3H, d, *J* 7.70 Hz, $CH_3OC_6H_4CHCH_3$), 0.90 (9H, t, *J* 7.99 Hz, CH_3CH_2Si), and 0.51 (6H, q, *J* 7.95 Hz, CH_3CH_2Si);^{13}C NMR (125 MHz, $CDCl_3$) 156.8 (CH_3OC), 138.4 (C *ipso*), 127.9 (C *ortho*), 113.6 (C *meta*), 55.3 (CH_3O), 25.8 ($CH_3OC_6H_4CHSi$), 15.8 ($CH_3OC_6H_4CHCH_3$), 7.5 (CH_3CH_2Si), and 2.2 (CH_3CH_2Si); ^{29}Si NMR (49.69 MHz, C_6D_6) 7.27 (s); GCMS (BP1 12m 140 °C room temperature 314 s, EI^+) *m/z* 250 (M^+); ν_{max} (thin film) 1611 cm^{-1} (C=C Ar). Anal. Calcd for $C_{15}H_{26}OSi$ C, 71.93; H, 10.46. Found: C, 72.03; H, 10.86.

Reaction of 1 with Triethylsilane. The following procedure is typical: A suspension of tetrakis(η^2 ethene)di-μ-chlorodirhodium (15.4 mg, 39.6 μmol) in C_6D_6 (200 μL) in a 1000-μL graduated flask, attached to the vacuum line under argon, was treated with 4-methoxyphenylethene **1** (20 mg, 20 μL, 0.149 mmol) to afford a deep red solution of complex **7**. The solution was accurately diluted to a total volume of 1.00 mL with C_6D_6. The resultant orange-red solution was transferred *via* a filtering cannula into a 1.5-mL vial under argon, and the vial was sealed with a septum cap. (4-Methoxyphenyl)ethene **1** (40 μL, 40 mg, 0.298 mmol) was added *via* microsyringe to a 1.5-mL ampoule attached to the vacuum line, under argon. C_6D_6 (330 μL) followed by Et_3SiH (50 μL, 36.4 mg, 0.313 mmol) were added *via* microsyringe. The resulting clear colorless solution was treated with a 38-μL aliquot of the solution of rhodium complex **7** under argon. The bright yellow solution gradually turned brown over 18 h. The solution was transferred *via* cannula into a 5-mm NMR tube attached to the vacuum line under argon; and the product distribution was estimated by ^1H NMR (500 MHz).

Acknowledgment. We thank the following companies for contributing to this work through our Research Fund for Homogeneous Catalysis: Andeno BV, BP Chemicals, Courtaulds, Great Lakes, Hovione, Johnson-Matthey, MSD, Shell (KSLA), Smith Kline Beecham, Quest, and Wyeth's. Dr. Tim Layzell and Dr. Erik Heeres made useful comments during the course of this work. Dr. Layzell made a careful critical reading of the manuscript.